Landslides (2018) 15:63–82
DOI 10.1007/s10346-017-0854-3
Received: 4 October 2016
Accepted: 19 June 2017
Published online: 15 July 2017

Antonio Santo · Giuseppe Di Crescenzo · Giovanni Forte · Raffaele Papa · Marianna Pirone · Gianfranco Urciuoli

Flow-type landslides in pyroclastic soils on flysch bedrock in southern Italy: the Bosco de' Preti case study

Abstract In the last 20 years, major efforts have been made to investigate shallow flow-type landslides. Such phenomena are usually rainfall-induced and in the geological context of Campania (Southern Italy) occur in pyroclastic soils resting on steep slopes mainly constituted by carbonate or volcanic bedrock and by flysch deposits. They are generally complex landslides with an early soil slide and a subsequent flow evolution. In this paper, a database of flowslides occurring in recent years within the flysch deposits of Avellino (Campanian Apennines) is first discussed and then the case study of Bosco de' Preti landslide on March 4, 2005, is described. The geological and geotechnical characteristics of the soils involved are described and the monitoring of the groundwater heads collected over 1 year from June 2005 to June 2006 is also shown. The last part of the paper illustrates the results of numerical modelling of the landslide triggering to gain insights into such phenomena. Slope stability analyses are preceded by hydrological modelling of the slope based on the monitoring data. Numerical analysis demonstrated that the rainfall during the 2 months preceding the event was able to fully saturate the pyroclastic cover and to establish positive pore water pressure at the depth of the surface of rupture, a soil condition never witnessed in carbonatic contexts. Hence, a combination of antecedent (predisposing factors) and single rainfall events (triggering factors) led to slope failure, as usually happens in pyroclastic soils in carbonatic and volcanic contexts. Finally, analysis of the historical landslides together with detailed investigation of the Bosco de' Preti case study permitted comparison between flow-type landslides in pyroclastic soils on carbonatic/volcanic bedrock and those on flysch.

Keywords Flow-type landslides · Flysch · Pyroclastic soil · Partially saturated slope · Campania (southern Italy)

Introduction

In the last 20 years, major efforts have been made to gain insights into shallow flow-type landslides, which frequently affect the region of Campania (southern Italy), causing extensive damage and resulting in loss of life (Calcaterra et al. 1997; Celico and Guadagno 1998; Del Prete et al. 1998; Di Crescenzo and Santo 1999; Cascini et al. 2000; De Vita 2000; de Riso et al. 2004).

Landslides classified as flow-type encompass several kinds of phenomena, which occur in both natural and man-made slopes with strongly heterogeneous physical and mechanical properties (Cascini et al. 2003). As pertains to the kinematics of such events, several differences can be identified in the triggering, evolution and depositional stages of the landslides. In Campania, these events were also classified as "debris avalanches or debris flows" (Revellino et al. 2004; Guadagno and Revellino 2005) or "flowslides" (Cascini et al. 2003; Cascini and Sorbino 2003; Cascini and Ferlisi 2003; Cairo and Dente 2003; Olivares and Picarelli 2006), given the material involved, the natural water content and the geometric and kinematic features (Hungr et al. 2001). In the case of flowslides, a major role is played by in situ fluidification of the soil (Musso and Olivares 2004), which can liquefy when saturated (Olivares and Picarelli 2001).

Such landslides are usually rainfall-induced and occur in pyroclastic soils resting on steep slopes mainly overlapping carbonate, volcanic bedrock and flysch deposits. In this regard, several papers have dealt with flow-type landslides in carbonate and volcanic contexts, focusing on the evaluation of the triggering susceptibility (Andriola et al. 2009), material properties, on the modelling of the triggering conditions, volume estimates (De Falco et al. 2012), run-out and relationships between water content in the soil and rainfall (Cascini et al. 2005; Olivares and Picarelli 2006; Damiano et al. 2012; Papa et al. 2013; Pirone et al. 2015a, b; Pirone and Urciuoli 2016, Pirone et al. 2016a, b). Several years of research on the topic have also shown that these soils are in partially saturated conditions even in the winter period. Hence, the failure could occur in correspondence of negative pore water pressures and should be analysed in the framework of partially saturated soil mechanics (Fredlund et al. 2013). The regime of pore water pressure in the soil is mainly controlled by contact with the underlying fractured carbonate bedrock, characterized by very high permeability, which drains infiltrating water toward the deep water table. Thanks to advancements in knowledge coming from several years of research, complex numerical analyses can now be performed on the hydraulic behaviour of the slopes subject to several rainfall events in order to forecast the triggering of this kind of flow-type landslides (Pagano et al. 2010; Pirone et al. 2016a).

However, few studies have focused on landslides in pyroclastic soils resting on flysch bedrock (despite their frequent occurrence in Campania), which affect infrastructures and road networks and result in damage and loss of life. This paper attempts to reduce this gap, identifying the main similarities and differences between flow-type landslides affecting geological settings made of carbonate and flysch, focusing on a well-documented case study in flysch: the Bosco de' Preti landslide, which occurred on March 4, 2005, in the Campanian Apennines in southern Italy.

The paper presents the main geomorphological features of landslides in similar geological settings ("Geological and geomorphological setting" section), especially the description of the March 4, 2005, event ("The Bosco de' Preti landslide" section) with the stratigraphic and geotechnical characterization of the soils recognized at the site ("Stratigraphic and geotechnical characterization" section). The methods adopted to study and analyse the Bosco de' Preti landslide are summarized in the "Methods" section and the results from the monitoring stage and numerical analyses are presented in the "Results and discussion" section. The geotechnical characterisation of the soil was enriched with the results from a test field examined in depth 10 km away from the case in question, in fact the two soils

involved were practically the same as coming from the same eruption. Finally, several considerations are made on the differences between pyroclastic flow-type landslides on flysch and on carbonate bedrock.

The study area

Geological and geomorphological setting

The study area shown in Fig. 1 is located in the NE sector of Campania, where the carbonate ridges and the flysch hills are covered by several metres of pyroclastic fall deposits (constituted by ashes and pumices) from the eruptions of the Somma-Vesuvius volcano (Rolandi et al. 2000). The carbonate bedrock (Cretaceous) is part of the stratigraphic unit of Mts. Partenio (Bonardi et al. 1988) and is crossed by major regional normal faults which originated the Avellino graben. The latter is overlain by Miocene–Pliocene deposits in flysch facies, the tuff layer of the Campanian Ignimbrite and several pyroclastic fall deposits. In the E and SE sector, marly-clayey deposits (Miocene–Pliocene) crop out: they constitute small ridges with a maximum elevation of 700 m a.s.l. (Mt. Le Croci, Mt. Termito), on which small urban settlements lie (i.e. Aiello, Contrada, Forino). The shallowest part of those slopes is covered by pyroclastic soils made of intercalations of pedogenised ashes, palaeosoils and pumices, generally several decimetres to a few metres thick (Rolandi 1997; Rolandi et al. 2000; Pareschi et al. 2002). Flow-type landslides in these successions have repeatedly affected some major urban settlements, namely Avellino, and some small towns in its province (Monteforte, Contrada and Forino). In fact, between January 1997 and March 2005, nearly 20 landslides more than 100 m long were triggered by rainfall in the area (see Table 1 and Fig. 1).

In Fig. 2, geological cross-sections of some of the landslides listed in Table 1 are shown. They allow critical slope values for triggering to be estimated at around 15°–20°, which is lower than those estimated for the same phenomena on carbonate ridges (Di Crescenzo et al. 2008). Furthermore, the landslide crowns are mainly located in morphological concavities, where the pyroclastic soil is thicker (1–3 m) and lie on the underlying marly–clayey bedrock, as shown in the stratigraphic logs of Fig. 3. In contrast to what is observed for flow-type landslides in carbonate ridges, the same in flysch are unaffected by natural and artificial cuts (Guadagno et al. 2003; Di Crescenzo and Santo 2005; Guadagno et al. 2005), and the zones of depletion are wider than the total dimension of the landslide. Although the reach angle (Heim 1882; Hsù 1975; Scheidegger 1973; Corominas 1997; Calcaterra et al. 2003) has very low values of around 9°–19° (see again Fig. 2), these

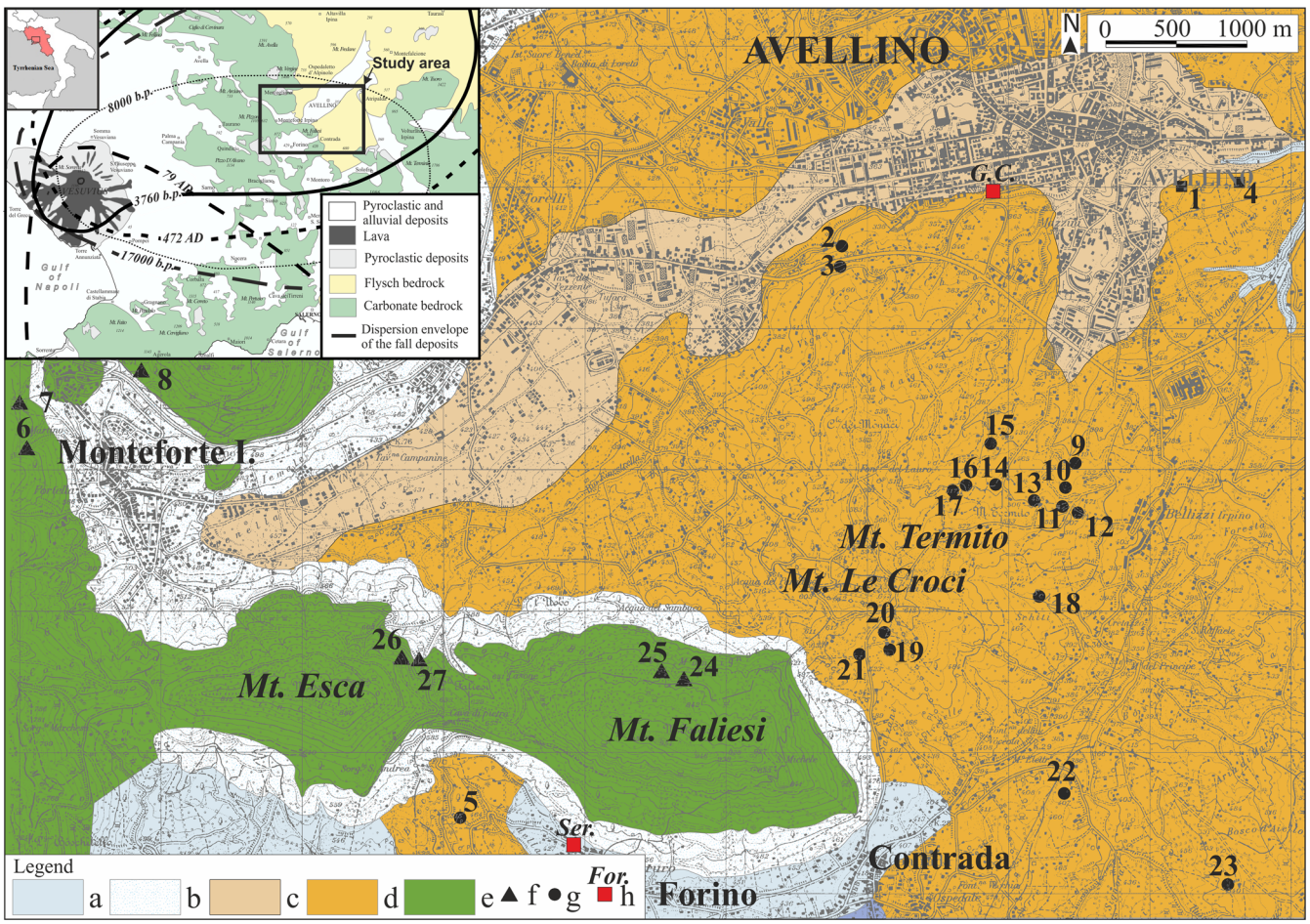

Fig. 1 Distribution of the main pyroclastic fall deposits of Somma-Vesuvius (data from Rolandi et al. 2000) and geological sketch of the study area with the location of the main landslides (see also Table 1). In the key: *a* recent alluvial deposits, *b* detrital deposits, *c* Campanian Ignimbrite, *d* Terrigenous Mio-Pliocene deposits, *e* cretaceous limestones, *f* flowslides on the carbonatic slope, *g* on the terrigenous slope, *h* rain gauges of Forino and Avellino

Table 1 Flow-type landslide inventory and main morphometric parameters (for the location in the plan, see Fig. 1)

ID	Area	Year	Bedrock	Crown height (m a.s.l.)	Length (m)	Reach angle (°)	Volume (m^3)
1	Avellino	1990	Conglomerate				
2	Avellino	1997	Flysch	367.5	19.5	13	1140
3	Avellino	1997	Flysch	398	23.4	22	543
4	Avellino	1997	Conglomerate				
5	Forino	1997	Flysch	521	54	11	19,500
6	Monteforte Irpino	1997	Limestone	750	175	23	6000
7	Monteforte Irpino	1997	Limestone				
8	Monteforte Irpino	1997	Limestone				
9	Avellino	2005	Flysch	442	37	18	950
10	Avellino	2005	Flysch	468	26	13	538
11	Avellino	2005	Flysch	509	41	16	2250
12	Avellino	2005	Flysch	495	15		198
13	Avellino	2005	Flysch	504	34	15	3264
14	Avellino	2005	Flysch	521	43	15	2130
15	Avellino	2005	Flysch	443	31	18	525
16	Avellino	2005	Flysch	515	18	13	625
17	Avellino	2005	Flysch	511	21	12	792
18	Avellino	2005	Flysch				
19	Avellino	2005	Flysch	557	37	12	5325
20	Avellino	2005	Flysch	578	21	14	2970
21	Avellino	2005	Flysch	564	24	15	5940
22	Contrada	2005	Flysch	442.5	69.5	9	6435
23	Aiello del Sabato	2005	Flysch	538	45	13	3400
24	Avellino	2005	Limestone	772	232	27	21,840
25	Avellino	2005	Limestone	775	255	26	14,175
26	Monteforte Irpino	2005	Limestone				
27	Monteforte Irpino	2006	Limestone				

phenomena present highly fluid bodies and velocities of around a few meters per second, which pertains to velocity classes 6–7 from the classification by Cruden and Varnes (1996).

The Bosco de' Preti landslide

The rainfall occurring between 4th and 5th of March 2005 strongly affected a small catchment in flysch (Mt. Le Croci), triggering three flowslides (19, 20, 21 from Table 1), as shown in Fig. 4. The events occurred on slope angles values between 10° and 20° in an area drained by small streams reaching the Sabato River. The main event (19), which occurred in the Bosco de' Preti area, is described in Figs. 5 and 6. It can be classified as a complex slide, initially triggered as a soil slide, which developed into a flowslide (Hungr et al. 2014). The main landslide crown formed on a mean slope angle of 16° and was located at 557 m a.s.l. The maximum length was of 180 m, with landslide toe located at 520 m a.s.l. affecting an overall area of 1400 m^2. The volume of pyroclastic soil mobilized was estimated by comparing previous and post-event aero-photogrammetric surveys, proving to be around 2700 m^3.

Interviews with local people permitted better description of the landslide evolution: the triggering stage was made up of two subsequent events, the first occurring around 2:00 pm and involving a volume of 1200 m^3, which reached the downslope stream with high velocity and swept a person walking on the down valley road for over 100 m (see again Fig. 5a). The second event followed at 4:00 pm and mobilized nearly 1500 m^3 of pyroclastic soil along the same path as the previous flowslide. Both phenomena started as soil slides along a surface of rupture between the pyroclastic cover and the clayey bedrock as shown in Fig. 5b, c. The initiation was followed by liquefaction and channelling of the mass. The phenomenon evolved into a flowslide, as demonstrated by flow traces located on the slip surface and on the flanks of the landslide. The mass was characterized by high fluidity and speed (several m/s). According to the descriptions provided by eyewitnesses and the

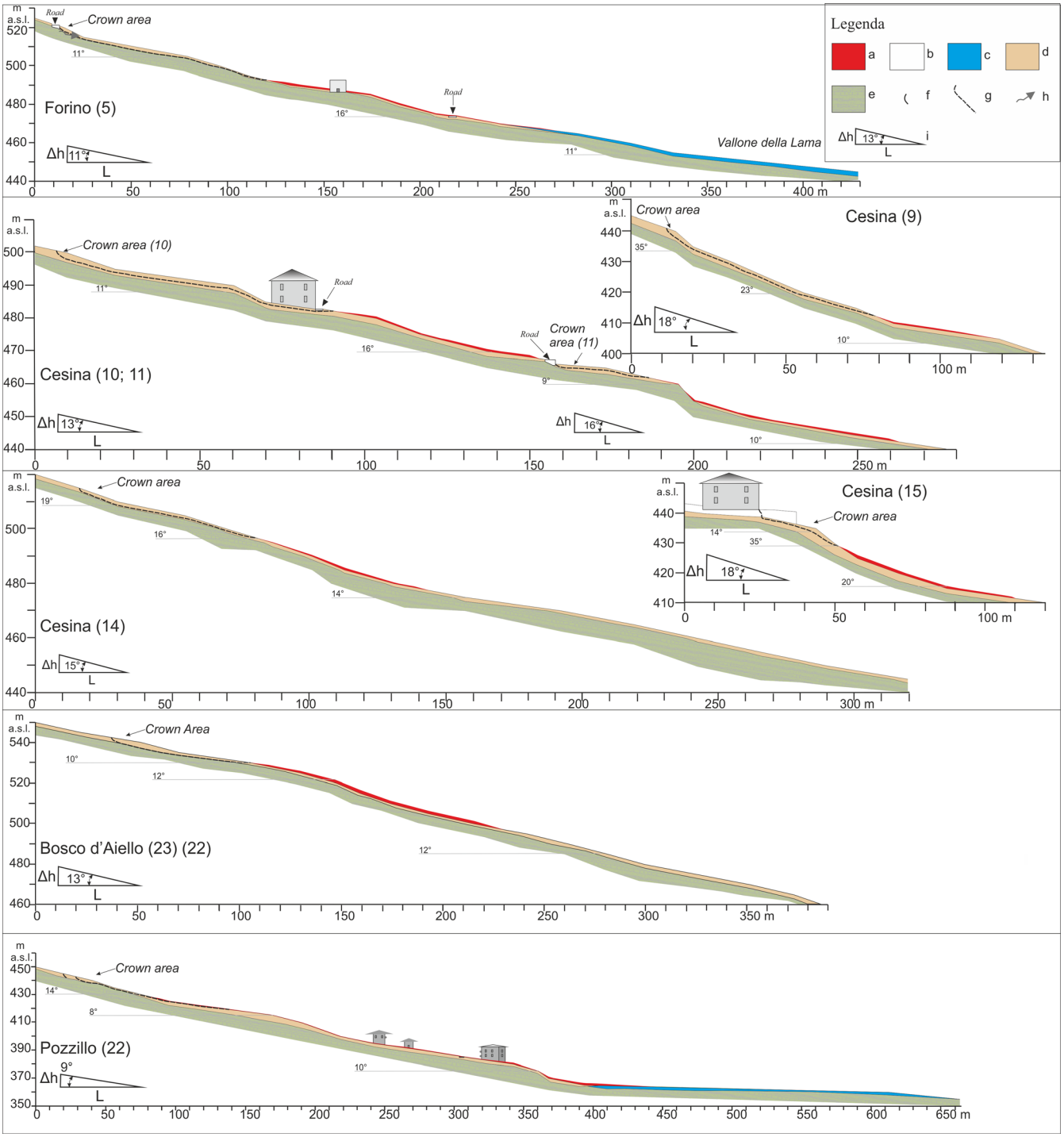

Fig. 2 Geological cross-sections of some of the landslides reported in Table 1. In the key: *a* landslide body, *b* reworked material, *c* recent alluvial deposits (Holocene), *d* reworked and weathered pyroclastic deposits (Holocene), *e* Miocene terrigenous deposits, *f* Joint, *g* rupture surface, *h* spring, *i* reach angles (modified from Di Crescenzo et al. 2008)

impact marks left on the walls of two houses, the height of the mud reached 1.2 m (Fig. 5e).

The impact was slightly inclined to the flow and the moving mass was characterized by a high water content. Indeed, greater damage would have been found at a lower water/solid ratio. Field surveys carried out in the aftermath of the event highlighted the presence of groundwater outflows in the crown and in the transition area (Fig. 5d). They were mainly located between the pyroclastic cover and the clayey bedrock. This evidence provides major insights into the groundwater regime and the role of pore pressures that were positive at the moment of triggering. By contrast, in carbonate contexts, landslides in pyroclastic soils are usually

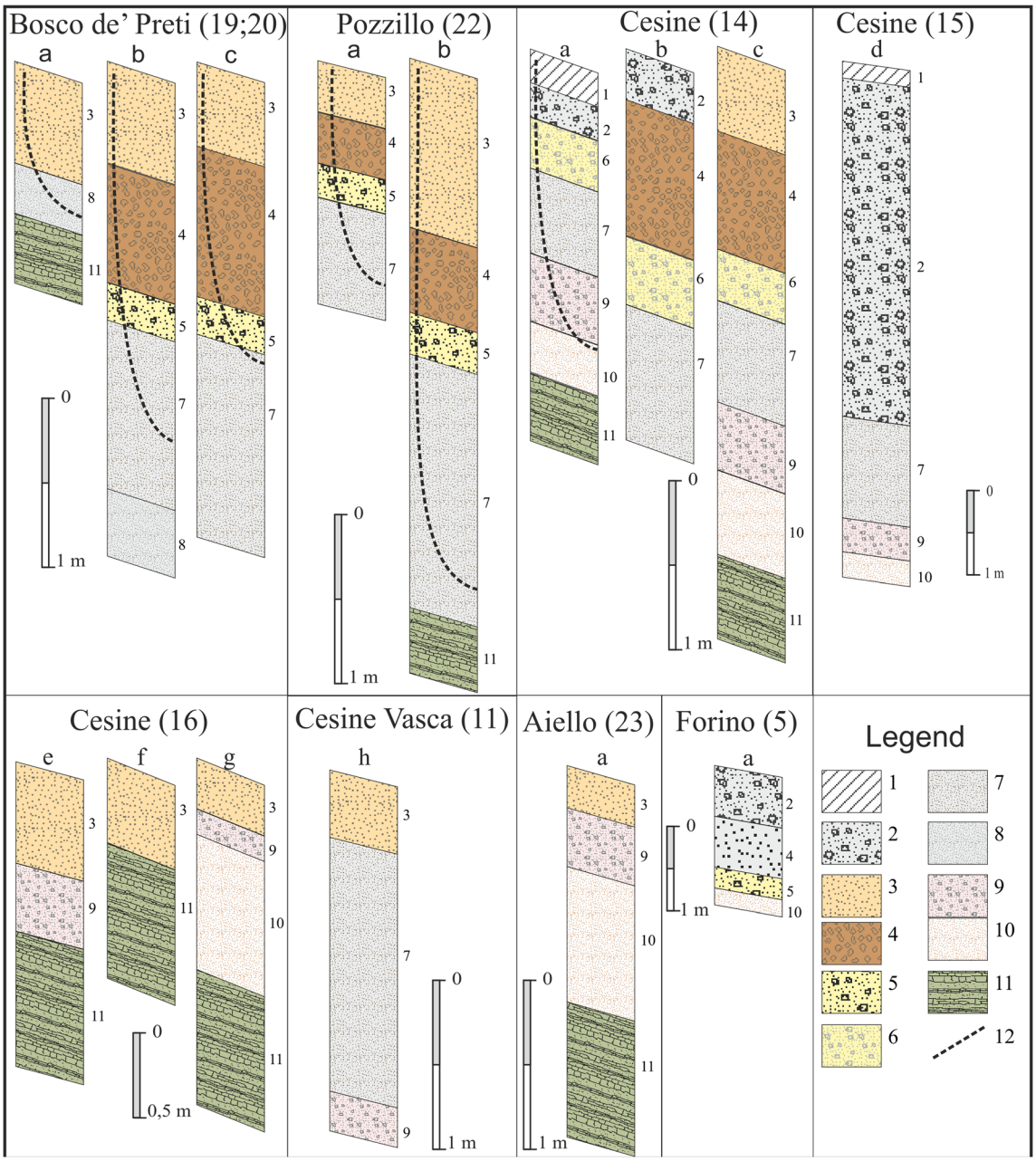

Fig. 3 Stratigraphic logs of the studied flowslides (see Fig. 1 for location on the plan). In the key: *1–2* reworked material, *3* actual pyroclastic soil with reworked pumices, *4* brown weathered fine-grained ashes with reworked pumices, *5* rounded white pumices (max. 3 mm) with a reverse graded bedding in sandy matrix (reworked material of the Avellino eruption), *6* pumice level of the Avellino eruption, *7* brown fine-grained ashes with reworked pumices, *8* weathered pyroclastic material with clay (palaeosoil), *9* pumice level of the Mercato eruption), *10* pyroclastic palaeosoil, *11* Marl with clay (Irpine Unit Flysch), *12* failure surface (modified after Di Crescenzo et al. 2008)

triggered in partially saturated conditions with negative values of pore water pressure.

Stratigraphic and geotechnical characterization

In order to identify the geological and geotechnical model of the landslide, an investigation campaign was carried out, consisting in seven boreholes, 4 SPTs, 6 CPTs and a collection of some undisturbed soil samples for the geotechnical characterization in the laboratory for both the pyroclastic soil cover and the underlying flysch bedrock. The above information allowed the identification of the stratigraphic setting of the materials involved in the landslide and the reconstruction of some detailed cross-sections of the slope topography before and after the event (Fig. 6).

The pyroclastic soils involved are partially saturated and their geotechnical behaviour was investigated in the framework of unsaturated soil mechanics (Fredlund et al. 2013). In this regard, in 2005, the authors chose to study and monitor a test site at the municipality of Monteforte Irpino (in Southern Italy) as representative of an area frequently affected by flowslides and characterized by a homogeneous pyroclastic cover. The latter mainly belong

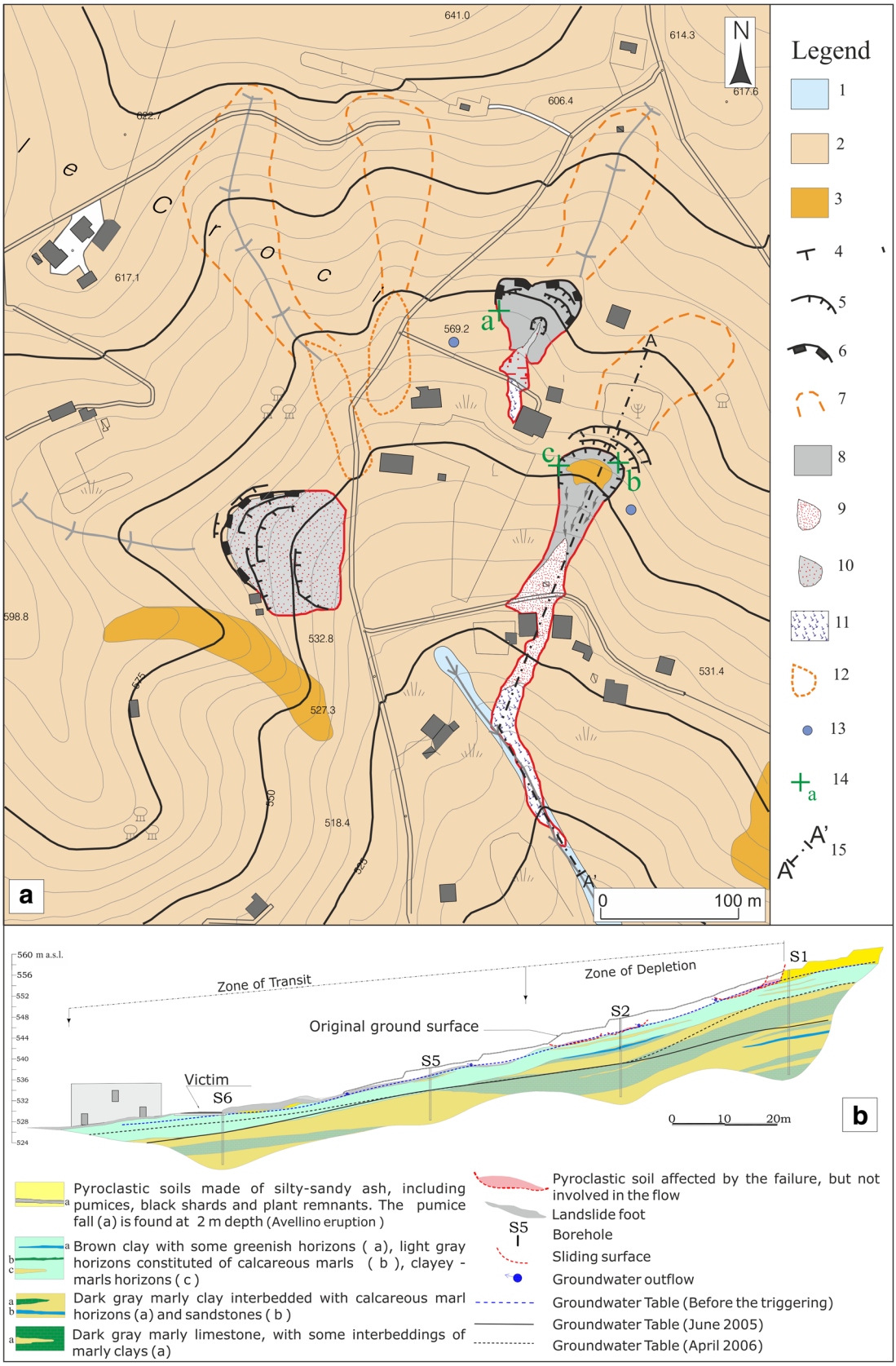

Fig. 4 Geological and geomorphological sketch of the area located on the southern slope of Mt. Le Croci). In the key: *1* recent alluvial deposits (Holocene), *2* pyroclastic deposits (Holocene), *3* Terrigenous Miocene deposits, *4* strata attitude, *5* main and secondary crown of the translational and *6* rotational slide, *7* ancient landslide, *8* triggering and sliding area, *9* landslide body of flowslide, *10* landslide body of rotational slide, *11* fluidification area of the landslide body, *12* ancient landslide body, *13* spring, *14* stratigraphic logs, *15* geological cross-sections

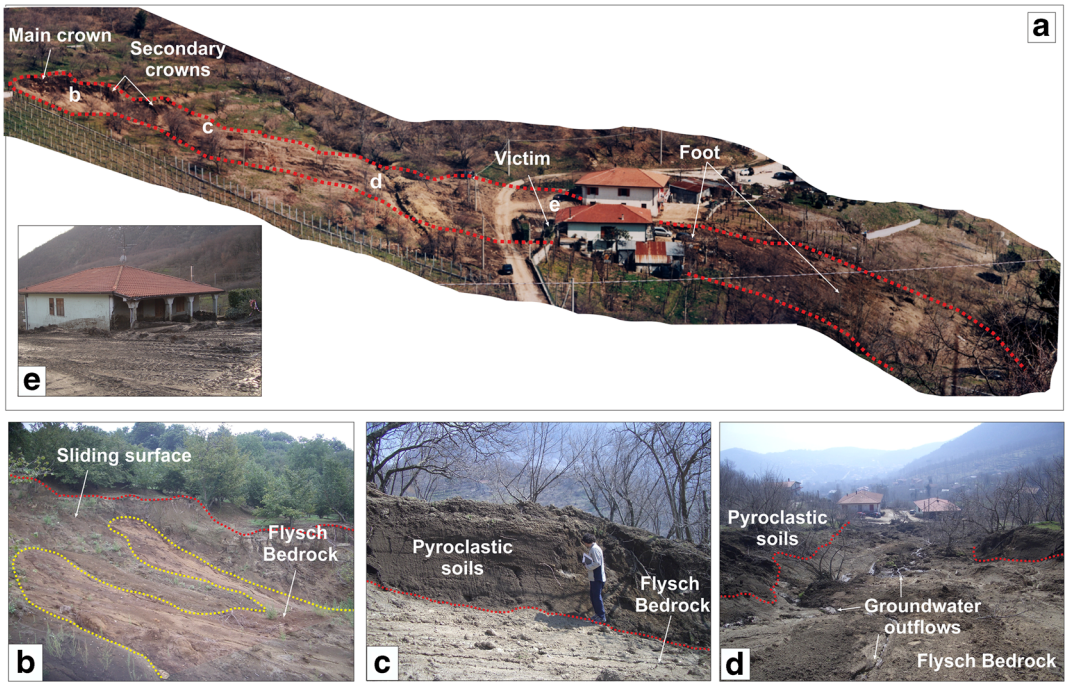

Fig. 5 March 4, 2005, Bosco de' Preti flowslide (modified after Di Crescenzo et al. 2008). **a** Overview of the flowslide and the affected area. **b** Detail of the crown showing the sliding surface and the outcrop of the flysch bedrock. **c** Lateral flank of the transition area. **d** Detail of the groundwater outflows. **e** Impact of the flow against the house

to the stratigraphic sequence of the Ottaviano eruption (8.0 ky BP). Their hydro-mechanical properties are well known to the authors, as they are the same soils characterized at the Monteforte Irpino test site, located at only 10 km from the site of Bosco de' Preti (Papa et al. 2013; Pirone et al., 2015a, b, c). At the test site of Monteforte Irpino, these soils are located below the pumices of the Avellino eruption at the depth of 2 m from the soil surface and they were well characterized by means of evaporation and drying tests and suction-controlled triaxial tests (Nicotera et al. 2010; Nicotera et al. 2015). In accordance with the above, the grain-size distribution of the samples collected in the area of Bosco de' Preti resulted completely contained in the grain-size envelope of the

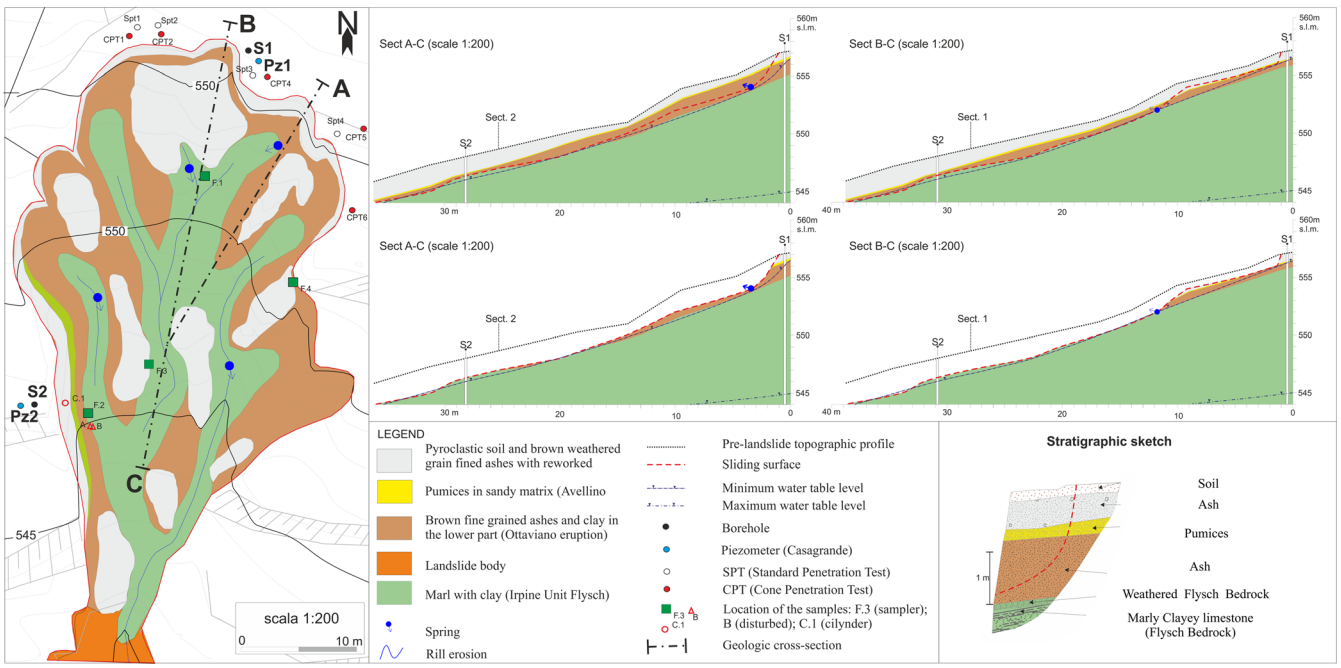

Fig. 6 Geological sketch map and cross-sections of the Bosco de' Preti depletion zone

soils of the Ottaviano eruption analysed in Monteforte Irpino (Fig. 7a). Henceforth, the same curves of soil water retention, hydraulic conductivity and value of the critical state of friction angle can be adopted (Fig. 7b, c).

These soils present (i) the typical hydraulic behaviour of coarse-grained soils with a low suction entry value (<10 kPa), (ii) a saturated hydraulic conductivity of about 1.2×10^{-6} m/s, and (iii) a friction critical state angle of 37°. The physical and hydro-mechanical parameters of the soil cover are summarized in Table 2.

The flysch bedrock consists of a bluish soil, although a yellow layer a few decimetres thick is sometimes recognized below the pyroclastic cover as products of alteration and oxidation processes of the bedrock. On the basis of the grain-size distributions, the bedrock can be classified as clay with silt (Fig. 7a); both "yellow" and "blue" clay showed a porosity ranging between 0.48 and 0.53, a plastic limit, w_P, between 26 and 31% and a liquid limit w_L, between 68 and 74%. Therefore, they can be identified as high plasticity inorganic clay (Table 2). Peak friction shear strength was obtained by performing some direct shear tests on the yellow and blue clay: the blue clay exhibited a friction angle of 19° and cohesion of 12 kPa (Table 2).

Methods

Monitoring

The investigation campaign was coupled with the analysis of rainfall measurements, as shown in Fig. 8. Data came from the rain gauge of the Genio Civile of Avellino, located at 383 m a.s.l., close to the Sabato River (see again Fig. 1). The study area has a Mediterranean rainfall regime, with a particularly long wet period stretching from Autumn to Spring. The average annual rainfall is around 1062 mm; the wettest month is usually November (198 mm), while the driest is July (24 mm).

In order to monitor the groundwater regime, eight piezometers, comprising five open pipe (p_1, p_2, p_3, p_4, p_5) and three Casagrande piezometers (p_{1c}, p_{2c}, p_{6c}), reaching the flysch deposit, were installed outside the landslide area in June 2005 (see again Fig. 6). The pipes ranged between 8 and 20 m long, the Casagrande piezometers between 3 and 4 m. In both types of piezometers, the level of the water table rising up into the tube was measured by lowering an ultra-sound probe inside. From the water level in Casagrande piezometers (labelled p_{1c}, p_{2c}, p_{6c} in Fig. 10b), the pore pressure heads at the depth of the cells could be measured. The pipe piezometers (p_1, p_2, p_3, p_4, p_5 in Fig. 10b) consist of a tube-drilled full-height; thus, the level of the water table measured in the tube is roughly related to the soil water table in the surrounding soil.

Numerical modelling

In order to model the "Bosco de Preti" landslide, some uncoupled hydro-mechanical analyses were performed. Infiltration analyses were carried out by the Finite Element Code, SEEP/W, to obtain the pore pressure distribution in the subsoil as a response to rainfall.

SEEP/W adopts Darcy's law and Richard's equation to analyse the water flow through both saturated and unsaturated soil; the finite element form of the two-dimensional seepage equation is derived by applying the Galerkin Method of weighted residual to

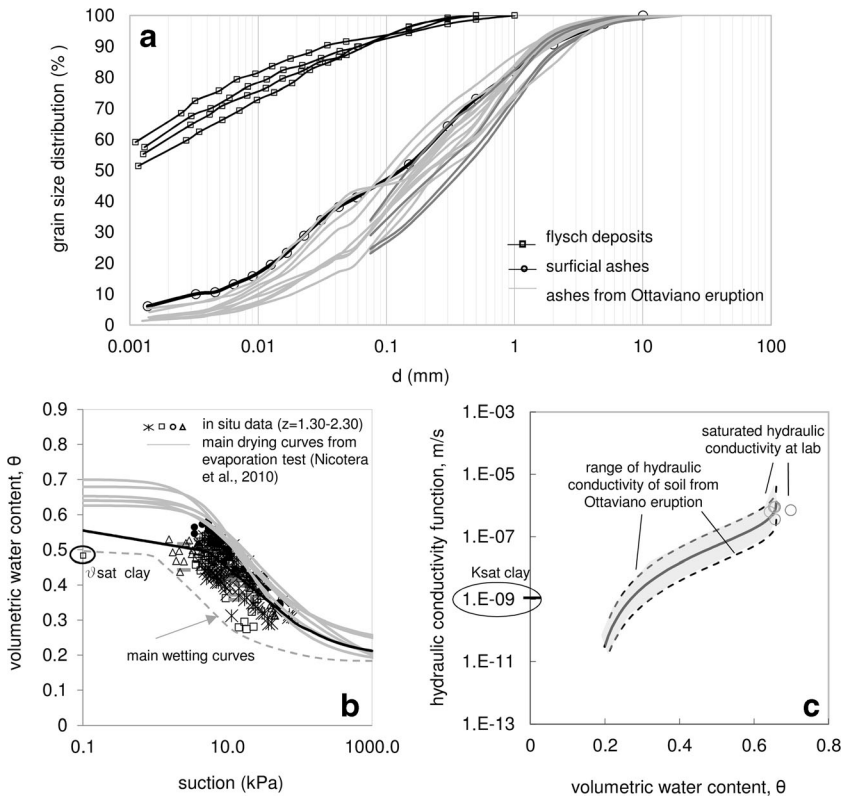

Fig. 7 Geotechnical soil characterization: grain-size distribution of the pyroclastic soil cover and flysch deposit recognized at site (**a**); soil water retention curves and hydraulic conductivity functions of the pyroclastic soil cover (**b**–**c**); hydraulic saturated conductivity of flysch deposit adopted in the numerical analyses (**c**)

Table 2 Soil physical, hydraulic and mechanical properties

Soil	γ_d kN/m^3	γ kN/m^3	Gs #	n #	Sr #	w_l #	w_p #	k_{SAT} m/s	ϕ' °	c' kPa
Ashes	7.11	12.11	2.62	0.71	–	–	–	1.2E^{-6}	37	0
Yellow clay	13.90	18.70	2.73	0.48	0.95	0.68	0.26	1.0E^{-9}	25	5.5
Blue clay	12.64	16.78	2.76	0.53	0.85	0.74	0.31	1.0E^{-9}	19	12

the governing differential equation, while the time integration is performed by a finite difference approximation scheme. The governing differential equation for two-dimensional seepage solved by the code is the following:

$$\frac{\partial}{\partial x}\left(k_x \frac{\partial H}{\partial x}\right) + \frac{\partial}{\partial y}\left(k_y \frac{\partial H}{\partial y}\right) + Q = \frac{\partial \theta}{\partial t} \quad (1)$$

where H is the total head, Q a possible internal source term, θ the volumetric water content, t the time and k_x and $k_y$the hydraulic conductivity in the x and in the y direction, respectively. The analyses were carried out by iterative equation solver and adaptive time stepping.

The hydraulic properties adopted for the pyroclastic soil were determined on the same soil located at 2 m from ground surface at Monteforte Irpino test site (Table 2), for which the authors collected a wide set of data from laboratory and field experimentation. These data define a wide hysteresis domain. All paths in the soil water retention plane are contained in the region delimited by the main drying and wetting curve, which are the upper and lower boundary, respectively, as represented in Fig. 7b. In particular, these are named scanning paths or intermediate curves characterized by negligible hysteresis (Fredlund, 2013).

The hydraulic characterization adopted in the analyses are reported in Fig. 9a–e, where the following curves are represented:

- (A): a scanning path and the hydraulic conductivity curve corresponding to the median saturated hydraulic conductivity (Fig. 9a–c);
- (B): a scanning path and the hydraulic conductivity curve corresponding to the maximum saturated hydraulic conductivity (Fig. 9a–c);
- (C): a scanning path and the hydraulic conductivity curve corresponding to the minimum saturated hydraulic conductivity (Fig. 9a–c);
- (D): the drying curve and the hydraulic conductivity curve corresponding to the median saturated hydraulic conductivity (Fig. 9d–f);
- (E): the wetting curve and the hydraulic conductivity curve corresponding to the median saturated hydraulic conductivity (Fig. 9d–f).

The hydraulic saturated conductivity of the flysch deposit was not investigated. Hence, a value of 1×10^{-9} m/s (Fig. 7c) was adopted, as equal to that measured on site in similar flysch deposits of the southern Apennines (Urciuoli et al., 2016a).

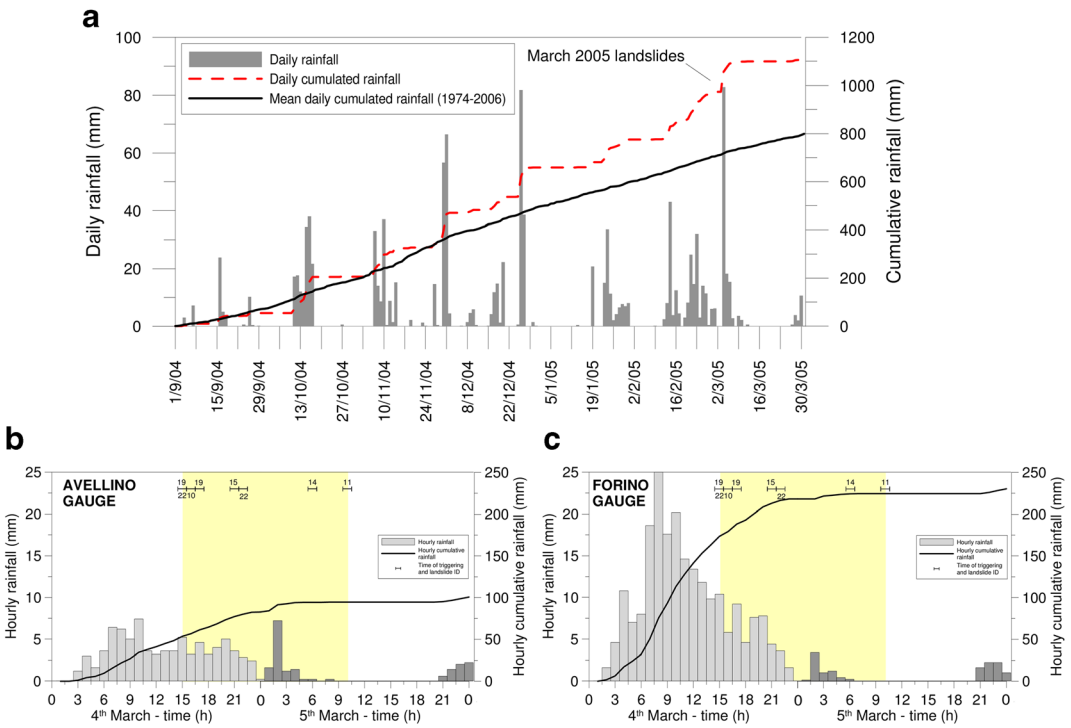

Fig. 8 Daily and cumulative rainfall (**a**), hourly and cumulative rainfall at Avellino (**b**), and Forino (**c**) rain gauges (modified after Di Crescenzo et al. 2008)

	Pyroclastic soil layer			clay soil layer
analysis	Soil water retention curve	Hysteretic Permeability curve (K-s)	Non-hysteretic Permeability curve (k-θ)	Saturated hydraulic conductivity (m/s)
(A)	Scanning curve	Scanning curve	Curve for median value of in situ saturated permeability	$1 * 10^{-9}$
(B)	Scanning curve	Scanning curve	Curve for maximum value of in situ saturated permeability	$1 * 10^{-9}$
(C)	Scanning curve	Scanning curve	Curve for minimum value of in situ saturated permeability	$1 * 10^{-9}$
(D)	Main drying curve	Main drying curve	Curve for median value of in situ saturated permeability	$1 * 10^{-9}$
(E)	Main wetting curve	Main wetting curve	Curve for median value of in situ saturated permeability	$1 * 10^{-9}$
(F)	Scanning curve	Scanning curve	Curve for median value of in situ saturated permeability	$1 * 10^{-10}$

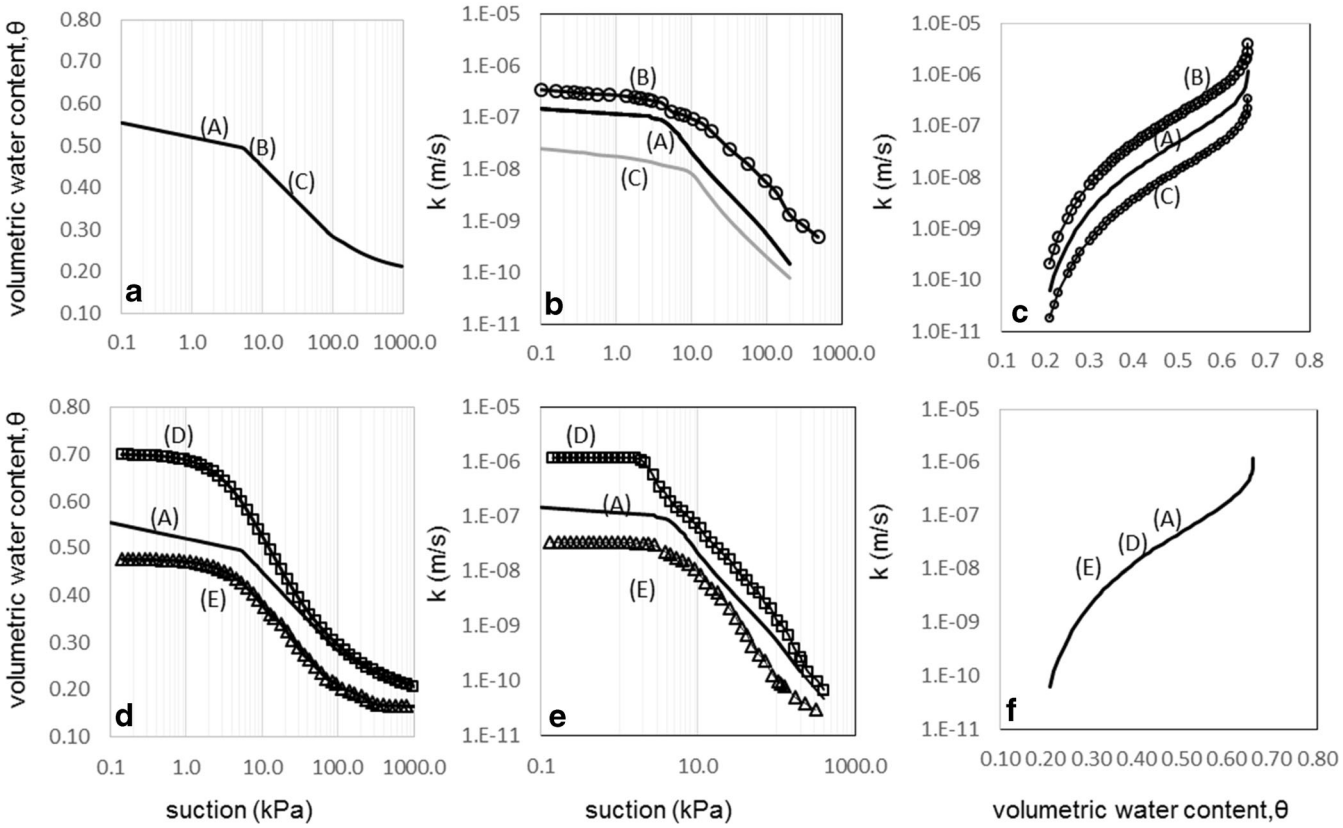

Fig. 9 Soil water retention curves (**a**, **d**) and hydraulic conductivity curves as a function of suction (**b**, **e**) and volumetric water content (**c**, **f**) adopted in all the analyses

The pore water pressure distribution calculated by SEEP/W at fixed time was adopted in the slope stability analyses carried out by means of the limit equilibrium method (LEM), using SLOPE/W. The apparent cohesion, c_a, when the suction establishes within the pyroclastic cover, was taken into account by using in SLOPE/W the extension of Mohr-Coulomb criteria to unsaturated soil. Nevertheless, this approach implies a fixed location of the rupture surface in advance and does not allow the development of the failure to be

followed. Furthermore, it is less time-consuming and requires fewer parameters than those needed to calibrate a constitutive law for unsaturated soil, like the Barcelona basic model, available in fully coupled model. In the examined case, the adopted procedure is particularly suitable because the shape and position of the rupture surface are known, being observed in the field. However, such an uncoupled approach consisting in the use of FEM for infiltration model combined with the LEM for slope stability analyses is widely used in the literature to model flow-type landslides. See for instance Collins et al., (2004), Rahardjo et al., (2007), Lu and Godt, (2008), Eichenberger et al., (2013), Springman et al., (2013), Zhang et al., (2014), Comegna et al., (2016b).

Results and discussion

Rainfall and groundwater regime

Figure 8a shows the daily and cumulative rainfall between 1 September 2004 and 30 March 2005. The cumulative rainfall of the mean annual rainfall evaluated from historical rainfall data between 1974 and 2006 (Fiorillo and Wilson 2004; Fiorillo and Revellino 2006) is reported too. In this regard, it is worth noting that starting from October 15, 2004, the cumulative rainfall exceeds the long-term averages in the same period (Fig. 8a).

Cumulative rainfall values are directly involved in triggering landslides, because they affect the soil pore water pressure prior to the event. In fact a distinction has to be made between *predisposing factors* identifying the slope and current soil conditions (morphology, stratigraphy, soil properties, suction and water content before the critical event) and *triggering factors* (critical rainfall sequence) which directly cause slope failure (Pirone et al. 2015a). The only reliable option for a good prediction or a good back analysis of landslide occurrence consists in assessing the current pore water pressure/suction of the soil which can lead to slope failure. Therefore, the seasonal pore pressure fluctuations are predisposing factors of slope instability (Pirone et al. 2015a). Knowledge of seasonal evolution of the corresponding *pore pressure* regime is extremely useful to evaluate the landslide susceptibility of the subsoil and to recognize the *most critical periods* and *unfavourable soil conditions* for slope stability in unsaturated pyroclastic soils. For instance, results from monitoring carried out at some unsaturated instrumented slopes in Campania (Comegna et al. 2016a; Pirone et al. 2015a) detect the most dangerous period for slope stability from January to April when critical steady conditions establish and suction attains values around 2–10 kPa in the whole pyroclastic cover.

As regards the critical precipitation, the daily rainfall around 101 mm recorded between 4 and 5 March 2005 by the Avellino rain gauge (Fig. 8b) was not exceptional (albeit considerable). The cumulative rainfall on the days preceding the event reached almost 100 mm at the Avellino rain gauge (Fig. 8b) and exceeded 200 mm at Forino (Fig. 8c). The peaks were recorded between 2:00 and 4:00 am on 5 March 2005. Maximum hourly peaks, however, occurred at 10:00 (7.4 mm/h) and 2:00 (7.2 mm/h), respectively, for the 4th and 5th at Avellino, and at 8:00 am (25 mm/h) for March 4 at the Forino rain gauge. The recorded peaks lie outside the time window of landslide triggering (yellow field in Fig. 8b, c) and precede the beginning of the landslide by about 5 h at Avellino and about 7 h at Forino.

During the post-event surveys, in the depletion area of almost all the landslides, groundwater outflow was observed for several days. This evidence indicates that the groundwater table was mainly located in the pyroclastic cover above the marl-clay soil of the flysch, which has a lower permeability than that of the pyroclastic soil. Hence, the loss of a portion of the cover due to the failure and topographic modification permitted groundwater outflow forming several ephemeral springs (see again Fig. 5d).

Daily and cumulative rainfall recorded by the Avellino rain gauge from June 2005 to June 2006 and the level of the water in the piezometers collected twice per month over the same period are reported in Fig. 10a, b, respectively. The measurements from Casagrande piezometers show seasonal oscillations of about 3 m: the minimum values are reached in August/September, the maximum in November/December (Fig. 10b). The amplitude of oscillations of the pore pressure heads at the depth of 3–4 m (2–3 m in Fig. 10b) agrees with findings in other flysch deposits (Urciuoli et al., 2016a, b). The amplitude of oscillations measured in pipe piezometers p_1, p_3 and p_4 exceeds 4 m (as much as 8 m) in 1 month. However, due to this type of piezometer, no definitive conclusions can be drawn about the water table in the soils. Nevertheless, it may be hypothesised that full saturation of the pyroclastic cover occurred around these open pipe piezometers (p_1, p_3 and p_4) and led to a considerable increase in the level of the water table in the tube.

The water level rise in the piezometers starts at the end of October and occurs after 198 mm of rainfall (total rainfall for November), close to maximum mean monthly values recorded from 1974 to 2006. Importantly, the increase from the end of October to mid−/end of November occurred very rapidly, which may be due to a preferential flow path in the system of discontinuities found throughout the flysch deposits (Urciuoli 1998; Urciuoli et al., 2016b; Cilona et al. 2016). During the winter, from December to April, average rainfall was around 100 mm/month and the water level in the piezometers was more or less constant. Thus, steady conditions established, as was found in other clayey and pyroclastic slopes during the wet period (Urciuoli et al., 2016b). Indeed, in that period, several springs were observed in the area hit by the landslide on 4 March 2005 where the flysch deposit outcrops, indicating a water table positioned above the contact between the pyroclastic cover and the flysch deposit, as indicated also by piezometer data.

Summing up, the groundwater regime that establishes in the wet period represents a predisposing factor also for these landslides; where a single heavy rainfall during the same period could trigger a landslide, as demonstrated in the pyroclastic cover resting on carbonate and volcanic contexts by Pirone et al. (2015a and c) and Urciuoli et al. (2016b).

Infiltration analyses

Investigation of the hydraulic response of the slope to rainfall infiltration is required to understand the triggering mechanism of flow-type landslides. Indeed, rainwater infiltration reduces the matric suction (negative pore water pressure) in unsaturated soils, thus decreasing the soil shear strength (Fredlund et al. 2013; Pirone et al. 2015a). In this regard, the hydraulic slope behaviour was investigated by means of a numerical model set up in the Finite Element Method code, SEEP/W (Krahn 2004).

The adopted slope reported in Fig. 11a is part of the longitudinal section A-A' already shown in Fig. 6. It consists of a 166-m-long slope at an inclination of 9°, for which an unstructured mesh was adopted with the element's shortest edge equal to 15 cm. Rainfall

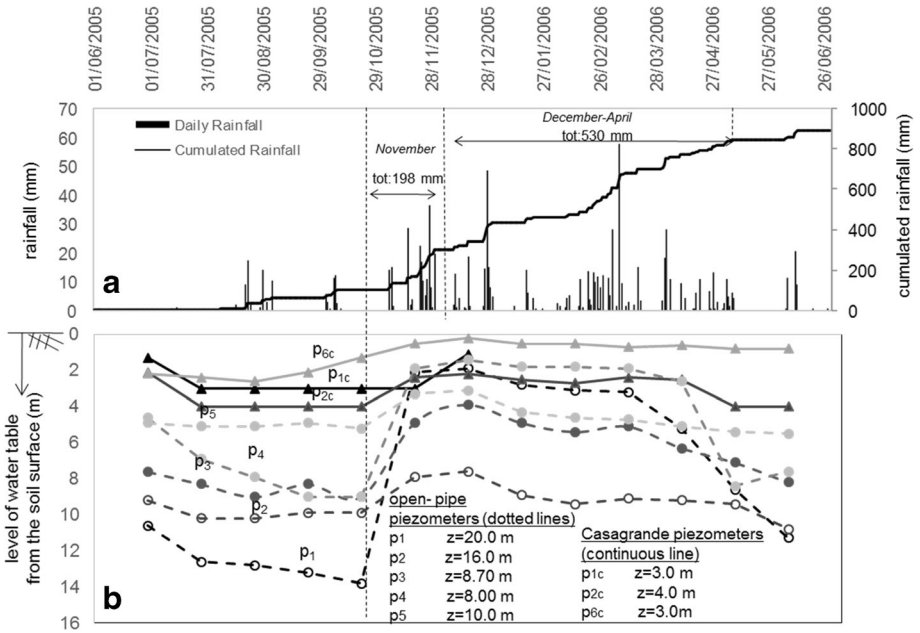

Fig. 10 Daily and cumulative rainfall from 1 June 2005 to 30 June 2006 (**a**). Water level measured in the open pipe piezometers and Casagrande piezometers installed outside the landslide (**b**)

measured in situ and crop evapotranspiration (Allen et al. 1998) over 1 year (Fig. 12b, c) were applied at the upper boundary of the analysed domain. Meteorological data available for the test site of Monteforte Irpino (10 km away from Bosco de' Preti) were used to

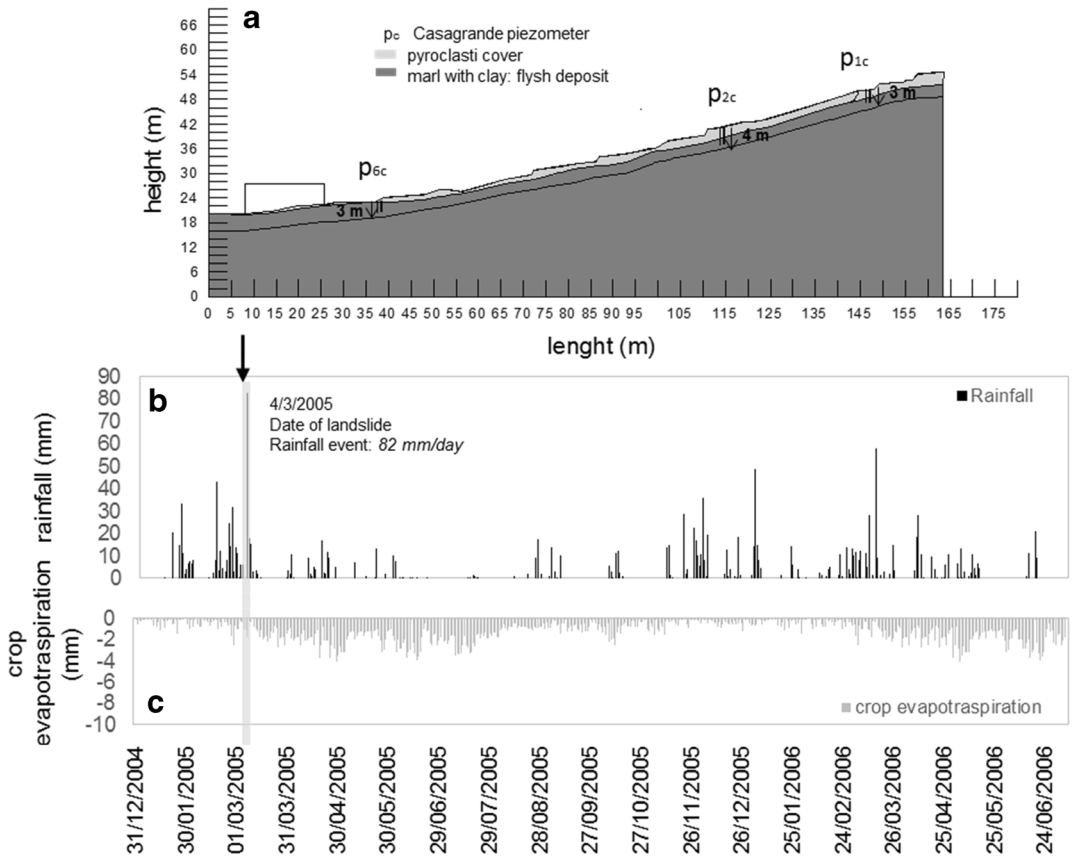

Fig. 11 Modelling of slope hydraulic behaviour: part of section a-a′ (Fig. 5a) with indication of piezometers (**a**), rainfall measured at site (**b**) and crop evapotranspiration (**c**) estimated from meteorological data recorded at Monteforte Irpino (AV) from 1 January 2005 to 30 June 2006

estimate crop evapotranspiration (Allen et al. 1998), assuming vegetation constituted of bushes.

A wide set of numerical analyses that differ for soil water retention curve and hydraulic conductivity function, according to the scheduled combinations from A to E (see the "Numerical modelling" section), was carried out in order to investigate the influence of the hydraulic properties of the pyroclastic soil layer upon the pore water pressure regime, and hence on the safety factor of the slope. All the analyses performed are summarized in the table reported in Fig. 9.

Pressure heads calculated in analyses A, B and C (which differ in the permeability function) at depths of 0.5, 1.8 and 4.0 m in the vertical section 2(s2c), and at the depth of 3.0 m in the vertical sections 1(s1c) and 6(s6c) are reported in Fig. 12a–e. Measurements in Casagrande piezometers are also overlaid on the pressure heads calculated at the same depths in the clay layer. Analysis (A) seems to provide the best fit between the pressure head calculated and those measured in Casagrande piezometers at the depth of 3.00 m (p_{1c}, p_{6c}) and 4.00 m (p_{2c}) from the soil surface, during the period from June 2005 to June 2006 (Fig. 12c–e). Moreover, this analysis provides compressive values of pore water pressure in the pyroclastic layer during the winter, even during the critical events of March 2005 according to what was discussed in the "Rainfall and groundwater regime" section. Analysis (C) returns smaller seasonal oscillation in pressure heads than that calculated by analysis (A) according to the lower conductivity adopted. Consequently, the pressure head calculated in analysis (C) does not at all match measurements in piezometers; in addition, tensile values of pore water pressure (suction) establish in the pyroclastic layer during the winter. With regard to analysis (B), seasonal oscillations in pressure heads exceed those calculated in the other two analyses (A and C), as expected due to the higher hydraulic conductivity

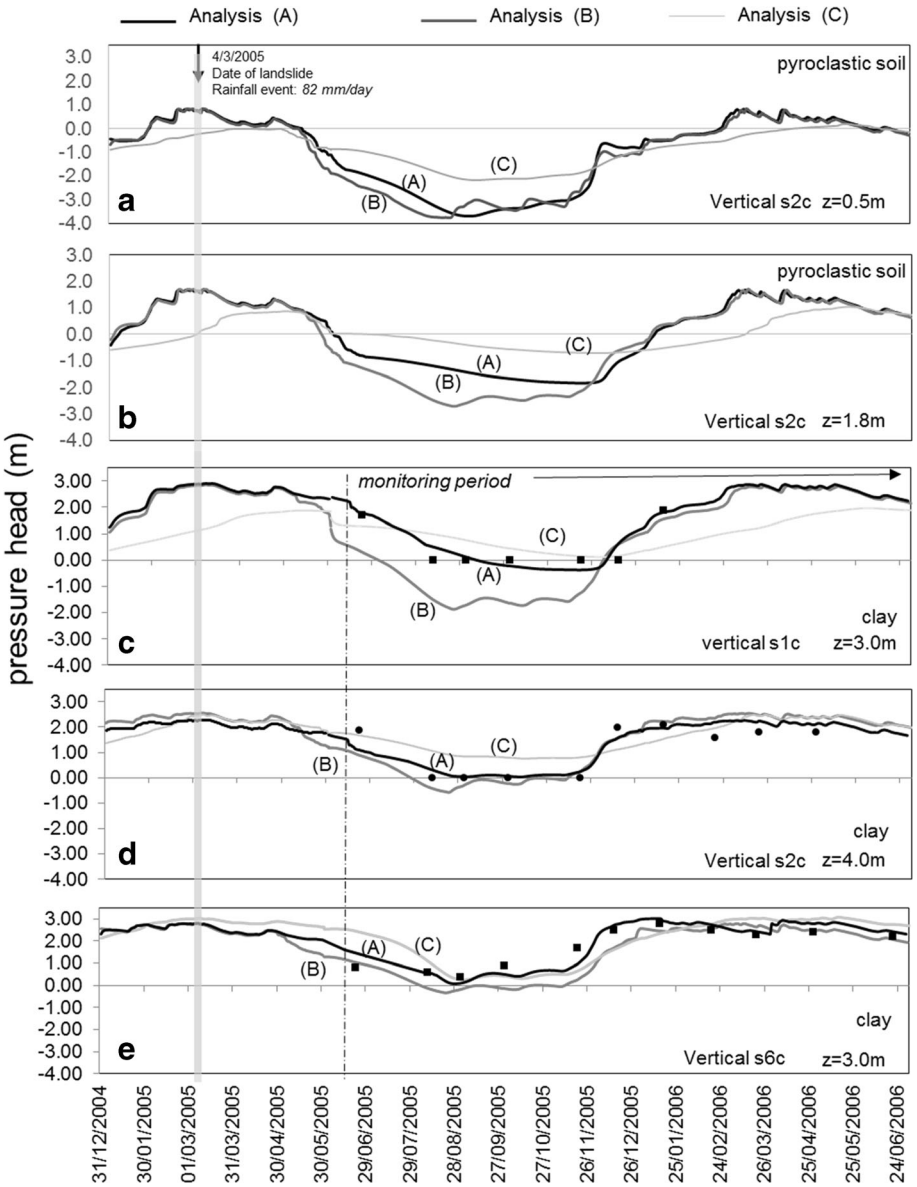

Fig. 12 Pressure heads calculated (*lines*) by SEEP/W in analysis *A*, *B*, and *C* at the vertical s2 at the depth of 0.5 m (**a**), 1.8 m (**b**), 4.0 m (**d**), at the vertical s1 at the depth of 3.0 m (**c**) and at the vertical s6 at the depth of 3.0 m (**e**). Pressure heads measured (*symbols*) in Casagrande piezometers at the depth of 3.0 m (**c**, **e**) and 4.0 m (**d**)

values used. In particular, during the dry period, the pressure heads fail to match the piezometer measurements well, while during the winter, they are comparable with those calculated in analysis (A). Therefore, the most suitable hydraulic conductivity curve should lie between the curves corresponding to the median and maximum value of in situ saturated conductivity. Nevertheless, it was verified that also the hydraulic conductivity curves corresponding to the saturated conductivity half an order of magnitude higher than the maximum measured at the Monteforte site (here used in analysis (B)) provide very similar results in the wet period. The median value of the permeability (A) is a threshold, beyond which the hydraulic response of the soil to the precipitations is quite fast and its transient phase quickly disappears (the distribution of pore water pressure in the soil is more or less steady).

Pressure heads calculated by analyses (A), (D) and (E) at the same depths investigated in Fig. 12a–e are reported in Fig. 13 a–e. This time, the analyses differ in soil water retention curves, thus, in conductivity curves too. The seasonal oscillation in pressure heads calculated by analysis (E) is smaller than the others according to the lower conductivity adopted, and the response to single events is very delayed. As regards analysis (D), the seasonal oscillation is always lower than that calculated in analysis (A) although the permeability values are higher than that used in analysis (A). This is probably due to the lower value of the water storage modulus (expressed as the arithmetic slope of the soil water retention curve) for the scanning path used in (A) with respect to the main drying curve adopted in (D). Therefore, observing the results in Fig. 13a–e, the proper soil water retention curve has to be represented by a scanning path close to that used in (A). These results

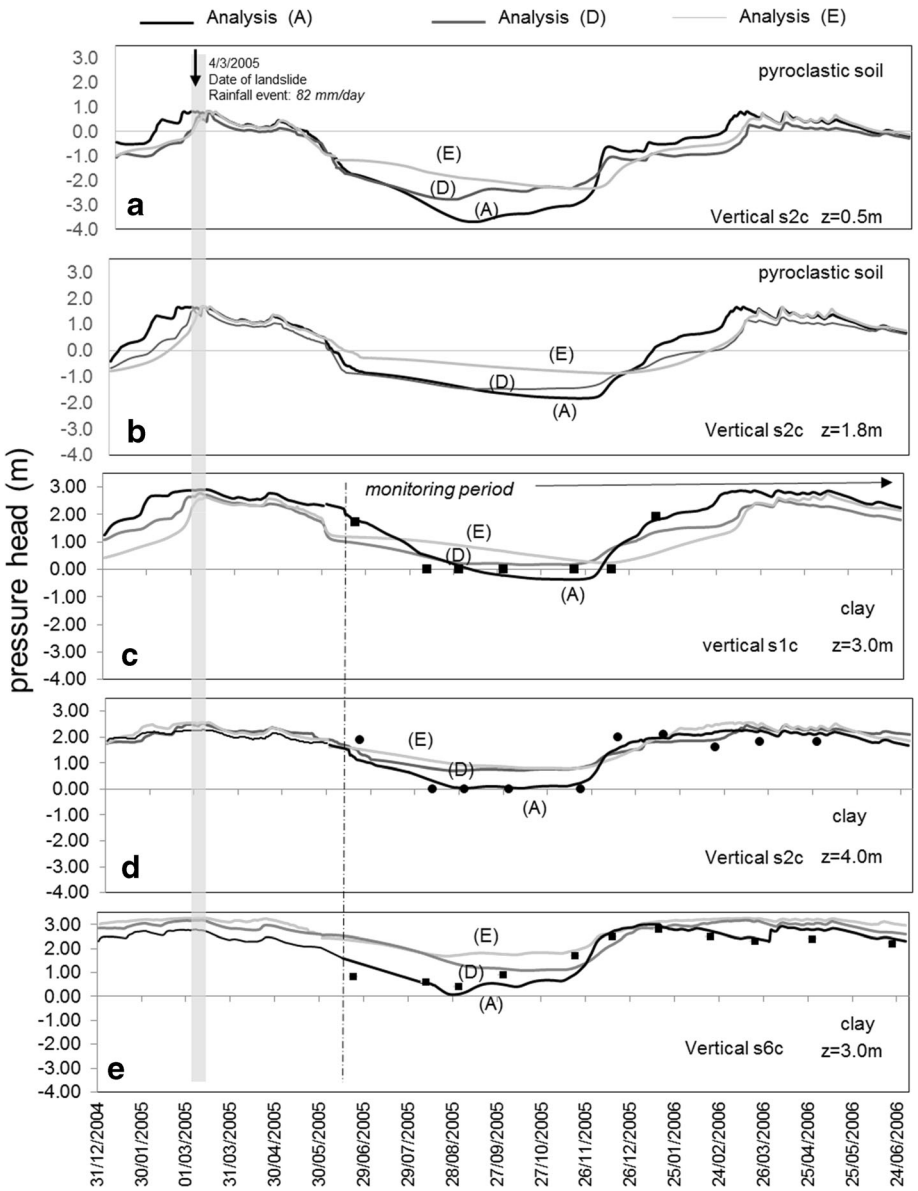

Fig. 13 Pressure heads calculated (*lines*) by SEEP/W in analysis *A*, *D*, and *E* at the vertical s2 at the depth of 0.5 m (**a**), 1.8 m (**b**), 4.0 m (**d**), at the vertical s1 at the depth of 3.0 m (**c**) and at the vertical s6 at the depth of 3.0 m (**e**). Pressure heads measured (*symbols*) in Casagrande piezometers at the depth of 3.0 m (**c**, **e**) and 4.0 m (**d**)

show that the capacity of the soil to store water reduces the amplitude of pore pressure fluctuations.

A further analysis, termed (F) (see the Table in Fig. 9), adopting the properties of analysis A for the pyroclastic layer and the saturated conductivity of 10^{-10} m/s for the clay layer was carried out to investigate to what extent the hydraulic properties of clay can influence the pore pressure regime. For brevity's sake the results of analysis (F) are not included, yet they suggest that the hydraulic saturated conductivity of clay does not affect the pore water pressure in the pyroclastic cover. They provide only a slight reduction of the seasonal oscillation in pressure heads in the clay layer due to the lower saturated conductivity adopted.

Summing up, in light of these results, the curves used in analysis (A) provide (i) the best fit between the pressure head calculated and those measured in Casagrande piezometers, (ii) the compressive value of pore water pressure in the pyroclastic layer during the winter at the depth of the slip surface, according to what was discussed in the "Rainfall and groundwater regime" section. In Fig. 14a, b, pore pressure heads against time, grouped by layer type (pyroclastic and clay), calculated in analysis (A) are reported. In particular, the numerical model well reproduced 3 m of seasonal oscillations in pore pressure heads together with a 3–4 m lower water table depth in July than in November in the clay bedrock. Seasonal oscillations of 4–5 m in pressure heads are calculated in the pyroclastic soil. A mean pore water pressure value of 12–15 kPa at the depth of 1.8 m and 6–8 kPa at 0.6 m is obtained over the winter from January to April during both 2005 and 2006.

In this regard, in Fig. 14c, a detail of pore pressure heads and rainfall over the wet period from January to April for both 2005 and 2006 is shown at the depth of the rupture surface, 1.4 m from soil surface. The steady conditions established in February during 2005 and in March 2006 due to a smaller amount of antecedent rainfall in 2006 compared with 2005. Mean pore pressure head over the steady period ranges between 0.8 m (8 kPa of pore water pressure) and 1.2 m (12 kPa of pore water pressure). The variations in pore pressure heads are reported in Fig. 14d to investigate the effect of single events.

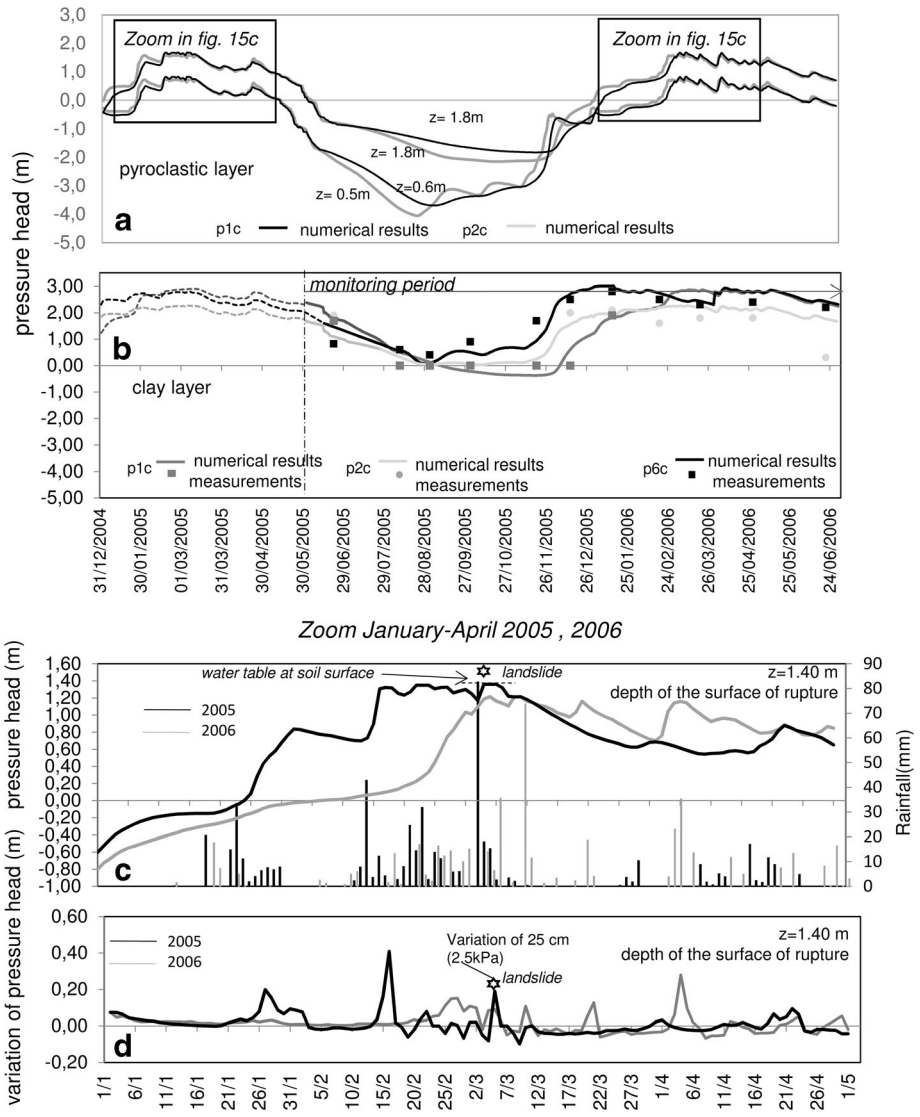

Fig. 14 Results of analysis (A): pressure heads calculated by SEEP/W code in the pyroclastic soils (**a**); comparison between pressure heads measured at Casagrande piezometers and those calculated by SEEP/W code in the clay layer (**b**); zoom on the period from January to April of both the years 2005 and 2006: pore pressure heads and daily rainfall over the same time interval (**c**) and daily variation in the pressure head at the depth of the slip surface (**d**)

In particular, the critical rainfall of March 4 caused a variation in pressure head of 25 cm (2.5 kPa) at the depth of the failure surface (1.40 m) and the water table rose to the ground surface. Some other intense rainfall events caused high oscillations that were even higher than that corresponding to the critical event (i.e. 16 February 2005 (0.4 m, 4 kPa)). However, none of these induced landslides due to the lower initial pore pressure soil condition (initial pore water pressure and volumetric water content).

Therefore, all the analyses show that seasonal fluctuations prevail over daily ones, as also observed in other monitored slopes in Campania (Urciuoli et al., 2016b). Hence, the predisposing factor plays a decisive role in landslide triggering.

Slope stability analysis

The numerical model discussed in the previous section was used to calculate pore water pressures from 1 January 2005 to 4 March 2005, adopting the hydraulic properties used in analysis (A). However, the same results were obtained by using those from analysis (B), in line with what was discussed above.

The pressure head values obtained were adopted in the Limit Equilibrium Method (LEM) implemented in the code SLOPE/W (Krahn 2004) to estimate the evolution of the safety factor along the observed rupture surface. The Morgenstern-Price method was adopted, the entry and exit of the slip surface were fixed in advance as envisaged by the LEM, and the minimum slip surface thickness was fixed at 0.5 m to avoid detecting very surficial failure.

The existence of a unique sliding surface located in the pyroclastic cover, triggered all at once, is not appropriate to justify the occurrence of the landslide. Indeed, the safety factor would always be higher than 1, even at the pore water pressure calculated on 4 March 2005. Therefore, in agreement with the evidence surveyed, two flowslides occurred, with the second activated after the first, as a consequence of the variation in topography induced by the first landslide (Fig. 16b, c).

Slope stability analyses were applied to the section B-C′ crossing the trigger area (Fig. 16a). The failure surface that detected the soil volume involved in the first trigger is traced in Fig. 16b: it is located on a steeper part of the slope and mainly crosses the pyroclastic layer. Only in a few points, it is in contact with the flysch deposit, according to the geological evidence observed after the events of 4th March (see Fig. 6). For the pyroclastic soil, the critical state friction angle of 37° was adopted (Table 2). Indeed, to take into account the apparent cohesion when the suction establishes within the soil cover, the

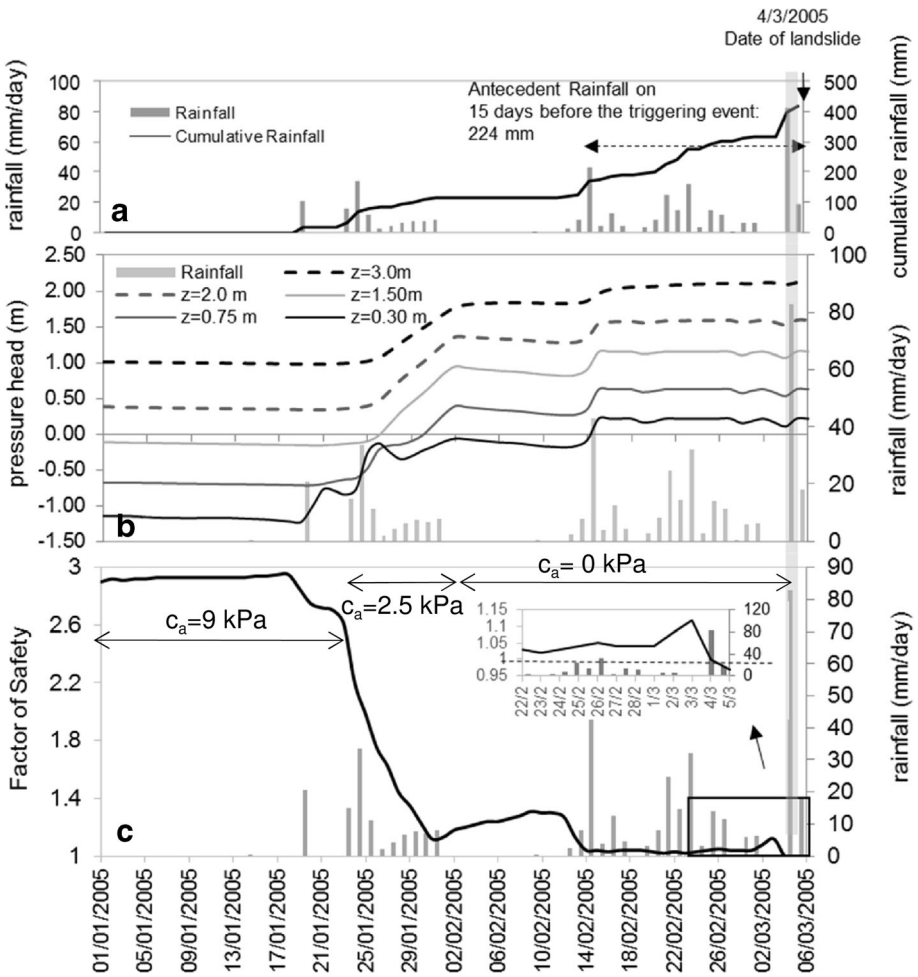

Fig. 15 Slope stability analyses: daily and cumulative rainfall measured at site (**a**); pressure head calculated at the depths of 0.30, 0.75, 1.50, 2.00 and 3.00 m (continuous lines indicate depths located in the pyroclastic layer and dotted lines in the flysch deposit) (**b**); safety factor calculated on the sliding surface shown in Fig. 16 over 2 months before the triggering event (from 1 January 2005 to 4 March 2006) with the mean values of apparent cohesion (Eq. 4) establishing within the pyroclastic cover (**c**)

extension of Mohr-Coulomb criteria to unsaturated soil was used in SLOPE/W (Fredlund et al. 2013):

$$\tau_f = c' + (\sigma_n - u_a) \times tan\phi' + (u_a - u_w) \times tan\phi_b \quad (2)$$

In Eq. (2), the term $\tan\phi_b$ is assumed equal to $S_r \tan \phi'$, and the degree of saturation S_r is detected on the soil retention curve adopted in the SEEP/W code in correspondence with the mean value of the calculated suction in the pyroclastic soil layer and adopting a porosity of 0.70. A Bishop effective stress approach (Bishop, 1959) was thereby implicitly adopted, with effective stress σ′ equal to:

$$\sigma' = (\sigma_n - u_a) + \chi(u_a - u_w) \quad (3)$$

and parameter χ equal to the degree of saturation.

The third term of Eq. (2), is the apparent cohesion, c_a:

$$c_a = (u_a - u_w) \cdot tan\phi_b = (u_a - u_w) \cdot Sr \cdot tan\phi' \quad (4)$$

For the flysch deposits, a peak shear strength was adopted (see Table 2) because no pre-existing slip surface was pointed out by previous geological investigation and the failure occurred mainly in the pyroclastic soil layer. Pore pressure heads calculated 2 months before the trigger events of 4 March 2005 at five different depths (z = 0.30, 0.75, 1.50, 2.00, 3.00 from the soil surface along a vertical section crossing the unstable volume) are reported in Fig. 15b. Safety factors corresponding to pore pressures calculated on a daily basis from 1 January 2005 up to 4 March 2005 are shown in Fig. 15c, together with the mean value of apparent cohesion, c_a, establishing within the pyroclastic cover.

The first 50 cm is partially saturated up to about 20–21st of January; hence the mean apparent cohesion, c_a, is approximately equal to 6 kPa and the safety factor is equal to 2.9. It is important to remark that in shallow landslides (where the thickness of the unstable cover is around 1–2 m) even such a low c_a value can allow the soil cover to be stable. After 120 mm of rainfall during the last week of January, all the pyroclastic soil cover becomes saturated apart from the first 30 cm (from soil surface) and the safety factor dropped to 1.15. During that period, c_a decreases from 6 to 0 kPa. Over the first 2 weeks of February, suction values within the first 30 cm increase slightly because evapotranspiration prevails over rainfall (Fig. 15a), while pore water pressures in the rest of the soil cover remain constant. The safety factor also increases slightly from 1.15 to 1.3. During the 2 weeks before the triggering event, 224 mm of rainfall fell and the whole pyroclastic soil cover became fully saturated, with the safety factor fluctuating between 1.05 and

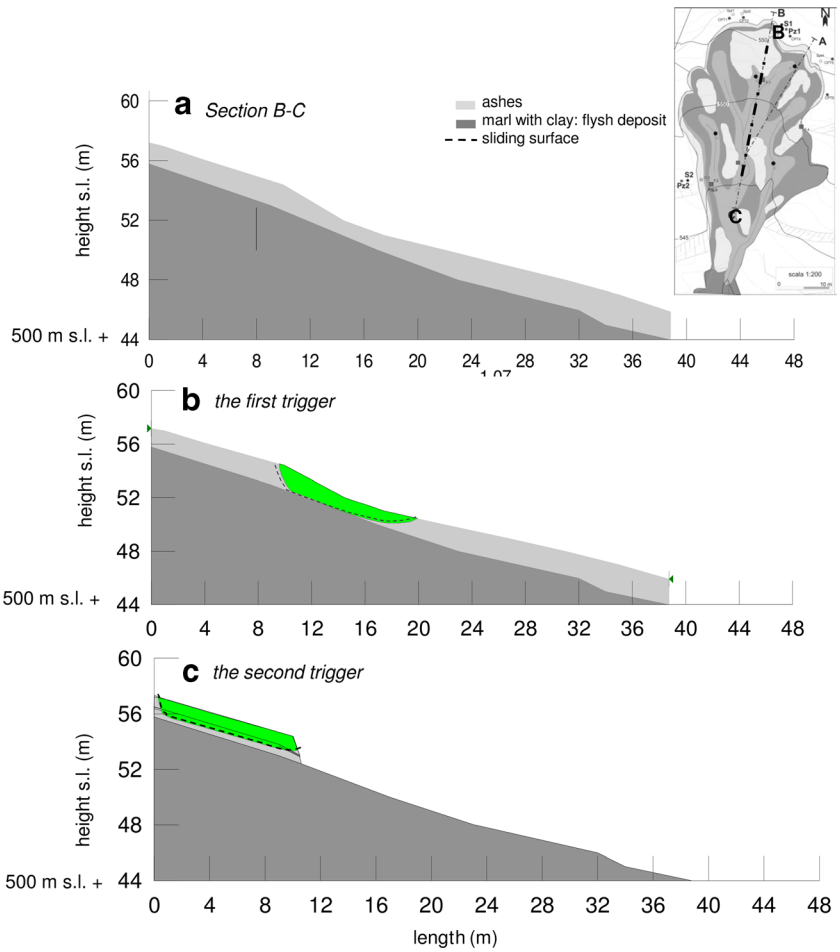

Fig. 16 Slope stability analyses: section crossing the triggering area (**a**); sliding surface relative to the first trigger (**b**) and the second trigger (**c**). The *green area* in panels **b** and **c** points out the unstable mass in the two critical events

1.03. Therefore, rainfall accumulating over 6 weeks prior to 4th of March allowed the increase in volumetric water content to saturation in the pyroclastic layer. Thus, this condition represented a predisposing factor to landslide. Meanwhile, 82 mm of rainfall concentrated in 1 day represented the triggering event able to lower the safety factor from 1.03 to below 1 (detail in Fig. 15c).

As recorded, 2 h after the first trigger there was a second trigger involving the zone upstream of the first crown. This situation was also investigated: a safety factor lower than one was obtained on the surface of rupture which completely crossed the pyroclastic volume no longer retained downslope (Fig. 16c).

These results show that flow-type landslides could occur in the pyroclastic cover resting on the flysch deposit with a slope angle of even less than 15° only if antecedent rainfall is able to fully saturate the cover and positive pore water pressures establish at the depth of the sliding surface. Importantly, during the winter, the rise in the groundwater table in the substratum up to the contact with the ash layer facilitates saturation of the soil cover. Hence, a similar combination of antecedent and single rainfall events could lead to failure in the pyroclastic cover resting both on fractured limestone with a slope angle exceeding 35° and on flysch deposits with a slope angle ranging on average between 15°–25°.

This case study in Campania can be considered representative of a large number of events which occur in other parts of Italy and worldwide: the conceptual model of the case study is that in which triggering involves a shallow permeable soil resting on an impermeable bedrock. It can be considered suitable also for crystalline bedrocks with their weathered cover (Li et al. 2016; Ietto et al. 2016; Schilirò et al. 2016; Pradhan and Kim 2015; Tsuchida et al. 2015) or in the eluvial and colluvial covers on clayshales (Berti and Simoni 2012; Panek et al. 2010; Mikoš et al. 2009; Picarelli et al. 2005).

Conclusions

This paper focuses on the Bosco de' Preti landslide (Avellino) which occurred on March 4, 2005, in the Campanian Apennines in southern Italy. It constitutes a case study of a complex landslide affecting pyroclastic soils on flysch bedrock. Such landslides are generally complex, characterized by an early slide and a subsequent flow evolution. The high fluidity and speed are noteworthy; the landslides present reach angles around 9° and 15° and can be triggered on gentle slopes (15°–25°). The rupture surfaces are generally located at the contact between the clayey-marly bedrock and the pyroclastic cover.

With regard to the case study presented here, some conclusions can be drawn:

- Fluidification definitely played a major role in both triggering and the run-out evolution. After the triggering, the mass was channelled into a small gully. According to the descriptions provided by eyewitnesses and the impact marks left on the walls of two houses, the height of the mud reached 1.2 m. The impact was slightly inclined to the flow and the landslide body had a high water content. Furthermore, the slide mass started in saturation conditions under positive pore pressures, as demonstrated by numerical analyses and the in situ evidence of the formation of ephemeral springs.
- From the monitoring data, the groundwater head in the clay layer showed seasonal oscillations of 2–3 m. A steady condition was established early on in the flysch deposit during the wet period from December to April of the years 2005 and 2006 (at a depth exceeding 2.5–3 m) and along with the antecedent total rainfall; this represented a predisposing factor for triggering the flowslide.
- From the infiltration analyses, the use of a scanning path and hydraulic conductivity function corresponding to the median value of in situ saturated conductivity (analysis A) provides the best fit between the calculated pressure heads and those measured in Casagrande piezometers; compressive pore water pressure values in the pyroclastic layer during the winter at the depth of the surface of ruptures. Rainfall during the months preceding the events was then able to fully saturate the cover and positive pore water pressures established at the depth of the sliding surface. Hence, a combination of antecedent (predisposing factors) and single rainfall events (triggering factors) could lead to the failure, as occurs on other slopes in Italy (Comegna et al. 2016b; Urciuoli et al., 2016b).
- Slope stability analyses appropriately reproduced the landslide occurrence and the results confirmed two distinct flowslide events, spaced a few hours apart, in agreement with the tell of local eyewitness.

Summing up, the hydraulic regime of the flysch interacts with the water circulation in the pyroclastic soil cover, as the presence of the water table at the lithologic contact facilitates saturation of the cover during the winter/spring. By contrast, for the triggering of pyroclastic layers resting on the fractured limestones, rainwater infiltrates the pyroclastic cover and drained off into the limestone toward the deeper groundwater table. Therefore, landslides of the discussed type involving flysch rocks can develop on less steep slopes (15°–25°) than those which develop in pyroclastic soils overlying limestone (35°). This consideration is relevant to the study of the susceptibility of the landslides involving pyroclastic soils on flysch bedrock or, generally, case studies where triggering involves a shallow soil much more permeable than the bedrock on which it rests.

Acknowledgements

The authors are grateful to the editor and the anonymous reviewers, whose suggestions and comments permitted marked improvements in the overall quality of the paper. Furthermore, the "Centro Funzionale per la Previsione Meteorologica e il Monitoraggio Meteo-Idro-Pluviometrico e delle frane della Regione Campania" is acknowledged for providing the rain gauge data.

References

Allen RG, Pereira LS, Raes D, Smith M (1998) Crop evapotranspiration: guidelines for computing crop requirements. Irrig Drain. 56, FAO, Rome, Italy

Andriola P, Chirico GB, De Falco M, Di Crescenzo G, Santo A (2009) A comparison between physically-based models and a semi-quantitative methodology for assessing susceptibility to flowslides triggering in pyroclastic deposits of southern Italy. Geogr Fis Din Quat 32(2):213–226

Berti M, Simoni A (2012) Observation and analysis of near-surface pore-pressure measurements in clay-shales slopes. Hydrol Process 26:2187–2205. doi:10.1002/hyp.7981

Bonardi G, D'Argenio B, Perrone V (Eds.) (1988) Carta geologica dell'Appennino meridionale alla scala 1:250.000. Mem Soc Geol It, 41, 1341, 1 tav

Cairo R, Dente G (2003) A flowslide in a pyroclastic soil fill. Proc. Int, Conf. on " fast slope movements—prediction and prevention for risk mitigation", vol 1. Patron Editore Bologna, Napoli, pp 93–100
Calcaterra D, Santo A, de Riso R, Budetta P, Di Crescenzo G, Franco I, Galletta G, Iovinelli R, Napoletano P, Palma B (1997) Fenomeni franosi in Penisola Sorrentina-Amalfitana connessi all'evento pluviometrico del gennaio 1997: primo contributo. Atti del IX congresso Nazionale dei Geologi, Roma, pp 223–231
Calcaterra D, de Riso R, Santo A, 2003. Landslide hazard and risk mapping: experiences from Campania, Italy. Atti del Convegno dell'Associazione Geotecnica Italiana; Napoli, 11–13 May 2003; Patron Editore Bologna
Cascini L, Guida D, Romanzi G, Nocera G, Sorbino G (2000) A preliminary model for the landslides of May 1998 in Campania Region. Proc. 2nd Intern. Symp. on Hard Soils Rocks: 1623–1649, Balkema
Cascini L Sorbino G (2003) Opere di protezione per i fenomeni di colata. Atti del XIX Ciclo di Conferenze di Geotecnica di Torino "Stabilità e Consolidamento dei Pendii"
Cascini L, Sorbino G, Cuomo S (2003) Modelling of flowslide triggering in pyroclastic soils. Proc. Int. Conf. on " Fast Slope Movements – Prediction and Prevention for Risk Mitigation". Napoli, Patron Editore Bologna 1:93–100
Cascini L, Ferlisi S (2003) Occurrence and consequences of flowslides: a case study. In: Picarelli L (ed) Proc. Int. Conf. on "fast slope movements, prediction and prevention for risk mitigation", vol 1. Pàtron Editore, Bologna, pp 85–92
Cascini L, Cuomo S, Sorbino G (2005) Flow-like mass movements in pyroclastic soils: remarks on the modelling of the triggering mechanism. Rivista Italiana di Geotecnica 4:11–31
Celico P, Guadagno F M (1998) L'instabilità delle coltri piroclastiche delle dorsali carbonatiche in Campania: attuali conoscenze, Quaderni di Geologia Applicata, 5–1, 75–133, Bologna
Cilona A, Aydin A, Likerman J, Parker B, Cherry J (2016) Structural and statistical characterization of joints and multi-scale faults in an alternating sandstone and shale turbidite sequence at the Santa Susana Field Laboratory: implications for their effects on groundwater flow and contaminant transport. J Struct Geol 85:95–114
Collins BD, Znidarcic D (2004) Stability analysis of rainfall induced landslides. J Geotech Geoenviron Eng ASCE 130(4):362–372
Corominas J (1997) The angle of reach as a mobility index for small and large landslides. Can Geotech J 33:260–271
Comegna L, Damiano E, Greco R, Guida A, Olivares L, Picarelli L (2016a) Field hydrological monitoring of a sloping shallow pyroclastic deposit. Can Geotech J 53(7):1125–1137
Comegna L, Damiano E, Greco R, Guida A, Olivares L, Picarelli L (2016b) Considerations on the failure of the Cervinara slope. Landslides and Engineered Slopes. Experience, Theory and Practice, 12th International Symposium on Landslides, 2016; Volume 2, 663–670, Napoli; Italy
Cruden DM Varnes DJ (1996) Landslide types and processes. In Turner A.K. & Schuster R.L. (eds.). Landslides: investigation and mitigation. Nat Res Counc, Transp Res Board Sp Rep 247, 36–75
Damiano E, Olivares L, Picarelli L (2012) Steep-slope monitoring in unsaturated pyroclastic soils. Eng Geol 137–138:1–12
De Falco M, Di Crescenzo G, Santo A (2012) Volume estimate of flow-type landslides along carbonatic and volcanic slopes in Campania (Southern Italy). Nat Hazards 61(1):51–63
de Riso R, Budetta P, Calcaterra D, De Luca C, Del Prete S, Di Crescenzo G, Guarino P, Mele R, Palma G, Santo A, Sgambati D (2004) Fenomeni di instabilità dei versanti dei Monti Lattari e dell'Area Flegrea (Campania). Quaderni di Geologia Applicata:11–11
De Vita P (2000) Fenomeni di instabilità delle coperture piroclastiche dei Monti Lattari, di Sarno e di Salerno (Campania) ed analisi degli eventi pluviometrici determinanti. Quaderni di Geologia Applicata 7:213–239
Del Prete M, Guadagno FM, Hawkins AB (1998) Preliminary report on the landslide of 5 May 1998, Campania, southern Italy—Bull. Eng Geol Env 57(1998):113–129
Di Crescenzo G, Santo A (1999) Analisi geomorfologica delle frane da scorrimento-colata rapida in depositi piroclastici della Penisola Sorrentina. Geogr Fis Din Quat 22:57–72
Di Crescenzo G, Santo A (2005) Debris slides-rapid earth flows in the carbonate massifs of the Campania region (southern Italy): morphological and morphometric data for evaluating triggering susceptibility. Geomorphology 66:255–276
Di Crescenzo G, Rotella M, Santo A (2008) Le frane da colata rapida in terreni piroclastici dei contesti in flysch dell'entroterra campano. Giornale di Geologia Applicata 8(2):193–215. doi:10.1474/GGA.2008-08.2-18.0210
Eichenberger J, Ferrari A, Laloui L (2013) Early warning thresholds for partially saturated slopes in volcanic ashes. Comput Geotech 49(2013):79–89
Fiorillo F, Wilson RC (2004) Rainfall induced debris flows in pyroclastic deposits, Campania (southern Italy). Eng Geol 75(3–4):263–289
Fiorillo F, Revellino P (2006) Le condizioni idrologiche che determinano lo sviluppo delle frane superficiali nell'area sannita: gli esempi del gennaio 2003 e del marzo 2005. Giornale di Geologia Applicata 3:129–136
Fredlund DG, Rahardjo H, Fredlund MD (2013) Unsaturated soil mechanics in engineering practice. Wiley-Interscience
Krahn J (2004) Seepage modeling with SEEP/W. Geoslope International Ltd.
Guadagno FM, Martino S, Scarascia Mugnozza G (2003) Influence of man-made cuts on the stability of pyroclastic covers (Campania-Southern Italy: a numerical modelling approach). Environ Geol 43:371–384
Guadagno FM, Forte R, Revellino P, Fiorillo F, Focareta M (2005) Some aspects of the initiation of debris avalanches in the Campania Region: the role of morphological slope discontinuities and the development of failure. Geomorphology 66:237–254
Guadagno F M Revellino P (2005) Debris avalanches and debris flows of the Campania region (southern Italy). In: debris-flow hazard and related phenomena. Matthias Jacob and Oldric Hungr (eds.), springer and praxis editorials
Heim A (1882) Der Bergsturz von Elm: Deutsch. Geol Gesell Zeitschr 34:74–115
Hsù KJ (1975) Catastrophic debris streams (Sturzstroms) generated by rockfalls. Geol Soc Am Bull 86:129–140
Hungr O, Evans SG, Bovis SG, Hutchinson JN (2001) A review of the classification of landslides of the flow-type. Environ Eng Geosci 7(3):1–18
Hungr O, Leroueil S, Picarelli L (2014) The Varnes classification of landslide types, an update. Landslides 11:167–194. doi:10.1007/s10346-013-0436-y
Ietto F, Perri F, Cella F (2016) Geotechnical and landslide aspects in weathered granitoid rock masses (Serre Massif, southern Calabria, Italy). Catena 145:301–315. doi:10.1016/j.catena.2016.06.027
Li WC, Dai FC, Wei YQ, Wang ML, Min H, Lee LM (2016) Implication of subsurface flow on rainfall-induced landslide: a case study. Landslides 13:1109–1123. doi:10.1007/s10346-015-0619-9
Lu N, Godt J (2008) Infinite slope stability under steady unsaturated seepage conditions. Water Resour Res 44:1–13
Mikoš M, Petkovšek A, Majes B (2009) Mechanisms of landslides in over-consolidated clays and flysch. Landslides 6:367–371. doi:10.1007/s10346-009-0171-6
Musso A, Olivares L (2004) Flowslides in pyroclastic soils—transition from "static liquefaction" to "fluidification". In L. Picarelli (ed.), Occurrence and mechanism of flows in natural slopes and earthfills, proceed. Int. Workshop, Sorrento, 14–16 May, 117–127, Patron Ed. Bologna
Nicotera MV, Papa R, Urciuoli G (2010) An experimental technique for determining the hydraulic properties of unsaturated pyroclastic soils. Geotech Test J (ASTM) 33(4):263–285
Nicotera MV, Papa R, Urciuoli G (2015) The hydro-mechanical behaviour of unsaturated pyroclastic soils: an experimental investigation. Eng Geol 195:70–84
Olivares L, Picarelli L (2001) Occurence of flowslides in soils of pyroclastic origin and considerations for landslides hazard mapping. Proceeding 14th South-east Asian Conf., Hong Kong, 881–886
Olivares L, Picarelli L (2006) Modelling of flowslides behaviour for risk mitigation. Proc. 6th Int. Conf. Physical Modelling in Geotechnics, Hong Kong. Taylor & Francis, London, 1, 99–112
Pagano L, Picarelli L, Rianna G, Urciuoli G (2010) A simple numerical procedure for timely prediction of precipitation-induced landslides in unsaturated pyroclastic soils. Landslides 7(3):273–289
Panek T, Hradecky J, Minar J, Silhan K (2010) Recurrent landslides predisposed by fault-induced weathering of flysch in the Western Carpathians. In: Calcaterra D, Parise M (eds) Weathering as a predisposing factor to slope movements. Geological society, vol 23. Engineering Geology Special Publications, London, pp 183–199. doi:10.1144/EGSP23.11
Papa R, Pirone M, Nicotera MV, Urciuoli G (2013) Seasonal groundwater regime in an unsaturated pyroclastic slope. Géotechnique 63(5):420–426
Pareschi MT, Santacroce R, Sulpizio R, Zanchetta G (2002) Volcanoclastic debris flows in the Clanio Valley (Campania, Italy): insight for the assessment of hazard potential. Geomorphology 43:219–231
Picarelli L, Urciuoli G, Ramondini M, Comegna L (2005) Main features of mudslides in tectonised highly fissured clay shales. Landslides 2:15–30. doi:10.1007/s10346-004-0040-2
Pirone M, Papa R, Nicotera MV, Urciuoli G (2015a) In situ monitoring of the groundwater field in an unsaturated pyroclastic slope for slope stability evaluation. Landslides 12(2):259–276
Pirone M, Papa R, Nicotera MV, Urciuoli G (2015b) Soil water balance in an unsaturated pyroclastic slope for evaluation of soil hydraulic behaviour and boundary conditions. J Hydrol 528:63–83. doi:10.1016/j.jhydrol.2015.06.005
Pirone M, Papa R, Nicotera MV, Urciuoli G (2015c) Hydro-mechanical analysis of an unsaturated pyroclastic slope based on monitoring data (book chapter). In: Lollino G, Giordan, D, Crosta, G, Corominas, J,Azzam R,Wasowski J,Sciarra N (Eds.), Engineering geology for society and territory, 2, landslide processes, 1069–1073

Pirone M, Urciuoli G (2016) Cyclical suction characteristics in unsaturated slopes. In: Volcanic rocks and soils - proceedings of the international workshop on volcanic rocks and soils, pp 183–184

Pirone M, Papa R, Nicotera MV, Urciuoli G (2016a) Analysis of safety factor in unsaturated pyroclastic slope. Landslides and Engineered Slopes. Experience, Theory and Practice: Proceedings of the 12th International Symposium on Landslides (Napoli, Italy, 12–19 June 2016) 3:1647–1654

Pirone M, Papa R, Nicotera MV, Urciuoli G (2016b) Hydraulic behaviour of unsaturated pyroclastic soil observed at different scales. Procedia Engineering 158(2016):182–187

Prahdan AMS, Kim YT (2015) Application and comparison of shallow landslide susceptibility models in weathered granite soil under extreme rainfall events. Environ Earth Sci 73:5761–5771. doi:10.1007/s12665-014-3829-x

Rahardjo H, Ong TH, Rezaur RB, Leong EC (2007) Factors controlling instability of homogeneous soil slope under rainfall. J Geotech Geoenviron Eng ASCE 133(22):1532–1543

Revellino P, Hungr O, Guadagno FM, Evans SG (2004) Velocity and runout simulation of destructive debris flows and debris avalanches in pyroclastic deposits, Campania region, Italy. Environ Geol 45:295–311

Rolandi G (1997) The eruptive history of Somma-Vesuvius volcanism and archaeology in Mediterranean area. De Vivo and Cortini.Ed

Rolandi G, Bertollini F, Cozzolino G, Esposito N, Sannino D (2000) Sull'origine delle coltri piroclastiche presenti sul versante occidentale del Pizzo d'Alvano (Sarno - Campania). Quad Geol Appl 7:37–47

Scheidegger AE (1973) On the prediction of the reach and velocity of catastrophic landslides. Rock Mech 5:231–236

Schilirò L, Montrasio L, Scarascia Mugnozza G (2016) Prediction of shallow landslide occurrence: validation of a physically-based approach through a real case study. Sci Total Environ 569-570:134–144. doi:10.1016/j.scitotenv.2016.06.124

Springman SM, Thielem A, Kienzler P, Friedel S (2013) A long-term field study for the investigation of rainfall-induced landslides. Geotechnique 63(14):1177–1193

Tsuchida T, Athapaththu AMRG, Hanaoka T, Kawaguchi M (2015) Investigation of landslide calamity due to torrential rainfall in Shobara City, Japan. Soils Found 55(5):1305–1317. doi:10.1016/j.sandf.2015.09.028

Urciuoli G (1998) Pore pressures in unstable scope constituted by fissured clay shales. In: Evengelista & Picarelli (Eds), the geotechnics of hard soils-soft rocks, vol 2. Balkema, Rotterdam, pp 1177–1185

Urciuoli G, Comegna L, Di Maio C, Picarelli L (2016a) The Basento valley: a natural laboratory to understand the mechanics of flowslides. Rivista Italiana di Geotecnica 50(1):71–90

Urciuoli G, Pirone M, Comegna L, Picarelli L (2016b) Long-term investigations on the pore pressure regime in saturated and unsaturated sloping soils. Eng Geol 212(2016):98–119

Zhang LL, Fredlund DG, Fredlund MD, Wilson W (2014) Modeling the unsaturated soil zone in slope stability analysis. Can Geotech J 51:1384–1398

A. Santo · G. Di Crescenzo · G. Forte (✉) · R. Papa · M. Pirone · G. Urciuoli
Dipartimento di Ingegneria Civile, Edile e Ambientale (DICEA),
Università degli Studi di Napoli Federico II,
Via Claudio 21, 80125, Naples, Italy
e-mail: giovanni.forte@unina.it